REPORT DOCUMENTATION PAGE	Form Approved OMB No. 0704-0188

1. AGENCY USE ONLY *(Leave blank)*	2. REPORT DATE	3. REPORT TYPE AND DATES COVERED
	[redacted]	DISSERTATION

4. TITLE AND SUBTITLE
PLASMA DEPOSITION OF OXIDE-COATED CATHODES

5. FUNDING NUMBERS

6. AUTHOR(S)
1ST LT UMSTATTD RYAN J

7. PERFORMING ORGANIZATION NAME(S) AND ADDRESS(ES)
UNIVERSITY OF CALIFORNIA AT DAVIS

8. PERFORMING ORGANIZATION REPORT NUMBER

9. SPONSORING/MONITORING AGENCY NAME(S) AND ADDRESS(ES)
THE DEPARTMENT OF THE AIR FORCE
AFIT/CIA, BLDG 125
2950 P STREET
WPAFB OH 45433

10. SPONSORING/MONITORING AGENCY REPORT NUMBER
FY99-38

11. SUPPLEMENTARY NOTES

12a. DISTRIBUTION AVAILABILITY STATEMENT
Unlimited distribution
In Accordance With AFI 35-205/AFIT Sup 1

12b. DISTRIBUTION CODE

13. ABSTRACT *(Maximum 200 words)*

14. SUBJECT TERMS	15. NUMBER OF PAGES
	16. PRICE CODE

17. SECURITY CLASSIFICATION OF REPORT	18. SECURITY CLASSIFICATION OF THIS PAGE	19. SECURITY CLASSIFICATION OF ABSTRACT	20. LIMITATION OF ABSTRACT

Ryan Jonathan Umstattd
September 1998
Applied Science

Plasma Deposition of Oxide-Coated Cathodes

Abstract

Vacuum arc deposition is employed to create a barium and/or strontium plasma which is subsequently deposited/implanted onto a nickel cathode substrate. The primary motivation for this work is the critical need for a reliable, repeatable, long-lived thermionic cathode for the production of high power, microsecond duration microwave pulses; such cathodes may also have applicability for lower current density continuous wave devices. This novel approach to manufacturing an oxide cathode eliminates the binders that may subsequently (and unpredictably) poison cathode emission. Removal of the poisoning mechanisms has yielded oxide cathodes capable of emission densities in the 20 A/cm^2 regime. Cathode lifetime and emission may be varied via the control over the deposition parameters such as coating thickness, implantation energy, and plasma stoichiometry. The deposition is performed by generating a cathodic arc discharge at the surface of a barium or barium-strontium alloy rod. The metal plasma thus created is then deposited on the substrate which can be negatively biased to encourage implantation during the deposition process. The deposition is performed with sufficient background oxygen present to oxidize the highly reactive metal coating. The plasma deposition is monitored via a rate thickness monitor, an optical emission spectrometer for plasma composition information, and an electrostatic Langmuir probe for the determination of the plasma density and temperature profile. Cathodes thus produced are analyzed by drawing pulsed current at a constant voltage for various values of decreasing cathode temperature in order to generate practical work function distributions which provide an indication of the quality and expected life time of the cathode.

Plasma Deposition of Oxide-Coated Cathodes

By

RYAN JONATHAN UMSTATTD
B.S. (Santa Clara University) 1994
M.S. (University of California, Davis) 1996

DISSERTATION

Submitted in partial satisfaction of the requirements for the degree of

DOCTOR OF PHILOSOPHY

in

Applied Science

in the

OFFICE OF GRADUATE STUDIES

of the

UNIVERSITY OF CALIFORNIA

DAVIS

Approved:

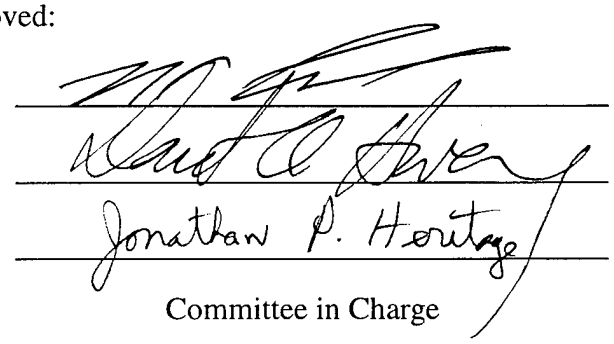

Committee in Charge

1998

Table of Contents

Acknowledgements:

This oxide cathode effort has been a joint University of California at Davis and Stanford Linear Accelerator Center (SLAC) project from the beginning. The assistance of personnel from both teams has been required throughout and much appreciated. The author would like to express special gratitude to Tao Pi, Ted Hillyer, Shaun McCaffery, Dr. Calvin Domier, and Prof. Neville C. Luhmann, Jr. of UC Davis as well as Bob Conley, Rich Callin, Dr. Glenn Scheitrum, and Dr. George Caryotakis from SLAC. In addition, George Miram was kind enough to give of his time and vast knowledge on the subject of cathodes.

This work is supported by the Air Force Office of Scientific Research under both the Advanced Thermionics Research Initiative (Grant F30602-94-2-001) as well as the Multidisciplinary University Research Initiative (Grant F49620-95-1-0253).

Ryan Jonathan Umstattd
September 1998
Applied Science

Plasma Deposition of Oxide-Coated Cathodes

Abstract

Vacuum arc deposition is employed to create a barium and/or strontium plasma which is subsequently deposited/implanted onto a nickel cathode substrate. The primary motivation for this work is the critical need for a reliable, repeatable, long-lived thermionic cathode for the production of high power, microsecond duration microwave pulses; such cathodes may also have applicability for lower current density continuous wave devices. This novel approach to manufacturing an oxide cathode eliminates the binders that may subsequently (and unpredictably) poison cathode emission. Removal of the poisoning mechanisms has yielded oxide cathodes capable of emission densities in the 20 A/cm^2 regime. Cathode lifetime and emission may be varied via the control over the deposition parameters such as coating thickness, implantation energy, and plasma stoichiometry. The deposition is performed by generating a cathodic arc discharge at the surface of a barium or barium-strontium alloy rod. The metal plasma thus created is then deposited on the substrate which can be negatively biased to encourage implantation during the deposition process. The deposition is performed with sufficient background oxygen present to oxidize the highly reactive metal coating. The plasma deposition is monitored via a rate thickness monitor, an optical emission spectrometer for plasma composition information, and an electrostatic Langmuir probe for the determination of the plasma density and temperature profile. Cathodes thus produced are analyzed by drawing pulsed current at a constant voltage for various values of decreasing cathode temperature in order to generate practical work function distributions which provide an indication of the quality and expected life time of the cathode.

I. INTRODUCTION

Vacuum arc plasmas and their peculiarities have been studied for over one hundred years. The first published paper on vacuum arcs was published in 1877 by Arthur Wright[1] who was one of the first three science Ph.D.'s to be produced by an American institution (Yale College). Thomas Edison applied for a patent[2] relating to the use of a continuous arc discharge (as opposed to a pulsed discharge) as a deposition scheme for manufacturing master molds of phonograms. Vacuum arcs were invented and reinvented many times during the following decades, but vacuum arc deposition was not industrially implemented until the 1970's in the former Sovient Union.[3] In addition to the deposition of thin films, vacuum arcs have a variety of applications including metal processing, vacuum switching of high current and high voltage, ion beam sources, and pulsed x-ray sources. An excellent review of these applications as well as the theory behind them was complied by R. L. Boxman, et al., in 1995,[4] and a very detailed bibliography of vacuum arc research literature was gathered by H. C. Miller in the late 1980's.[5] In the current work, vacuum arc deposition is used to deposit roughly a micron of barium oxide (or a barium-strontium oxide mix) onto a cylindrical nickel button 3.57 mm in diameter (0.1 cm^2 area) in the pursuit of a reliable, repeatable oxide-coated cathode (hereafter, oxide cathode).

The oxide cathode is a thermionic electron emitter that has been developed and employed since its discovery in 1903.[6,7,8] Oxide cathodes have found a variety of applications including flourescent lamps, monitor CRT's, satellite communications tubes,

and numerous other microwave tube devices. The traditional oxide cathode manufacturing process either paints or sprays a barium-strontium carbonate emission layer onto a nickel cathode base. The carbonate powders are mixed with nitrocellulose binder to provide adhesion to the nickel surface. In order to activate the cathode, the nitrocellulose must be burned off and the carbonates converted to oxides by heating the cathode and drawing current in vacuum. The activation process deposits byproducts on nearby surfaces which may act as cathode poisoning agents if they are later released due to electron beam interception or any other energetic event. An early experiment was performed by Sperry[9] in which the activation was performed in a separate chamber with the cathode subsequently mounted in a clean gun structure. The pulsed emission current from the experimental cathode exceeded 100 A/cm^2 compared to 15 A/cm^2 for the standard oxide cathode. The variability of both the coating process as well as the subsequent poisoning have prevented the successful manufacturing of a repeatable, reliable, high current density oxide cathode.

Oxide cathodes have always had attractively low work functions, but they have been plagued by the aforementioned variability in performance. Fig. I.1[10] is a comparison of the performance of various thermionic emitters in terms of their practical work function distributions. Clearly, a reliable oxide cathode holds the most promise for achieving high current densities at low operating temperatures which translates into a lower cathode heater power consumption and a longer cathode lifetime).

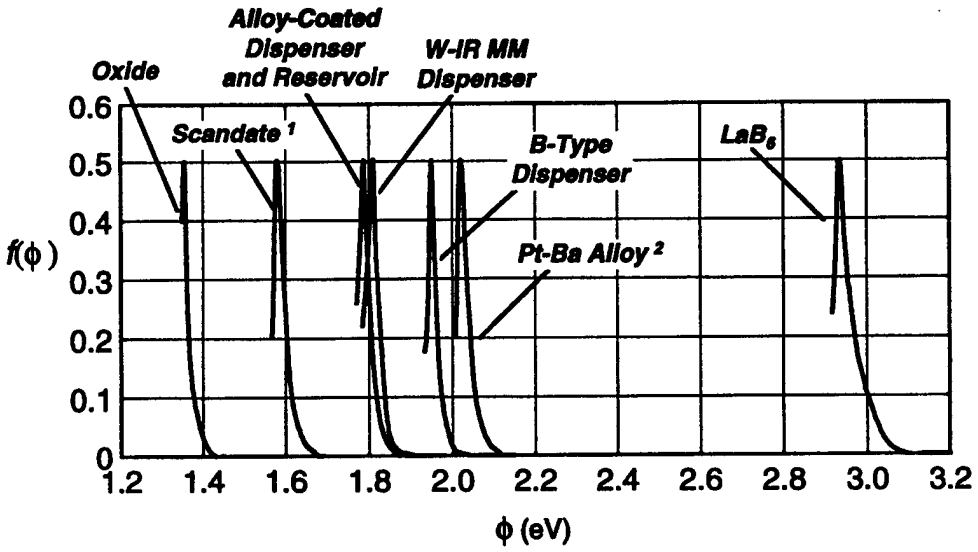

Fig. 1 Practical work function distribution for various thermionic cathode types. Data from CPI cathode life tests except (1) Deckers (Phillips, Netherlands) and (2) Djubua (Istok, Russia). After Cattelino and Miram.[10]

A definitive understanding of the chemistry of oxide cathode emission has yet to be achieved. The widely accepted model of high current density flow through the oxide coating relies on electron conduction through the pores in the coating left behind when the carbonates are converted into oxides;[11] however, Russian work on molecularly-deposited (most likely via a vapor deposition process) and pressed-porous oxide cathodes (the traditional coating is compressed after activation to increase the coating density) has led to equal, if not improved, emission characteristics without the presence of the electron gas-filled pores.[12] These encouraging results for nonporous oxide coatings, combined with the promise of a repeatable process for depositing a precisely controlled oxide coating, make a vacuum arc-deposited oxide cathode an exciting alternative to the traditionally spray-coated oxide cathode.

In the current work, vacuum arc deposition is employed to deposit barium and strontium oxides to make oxide cathodes developing a repeatable yet adjustable process. A multitude of process variables are monitored so that consistent results may be ensured. Cathodes thus produced are then tested for emission and have proven capable of pulsed current desities up to 20 A/cm^2 with practical work functions on the order of 1.6 eV. Thus, this plasma-deposited oxide cathode can emit 20 A/cm^2 pulsed at a temperature of only 900°C whereas the best dispenser cathode would require a temperature of over 1030°C to accomplish the same pulsed emission density. The primary future goal of this work is to improve the vacuum conditions under which the deposition and test of the oxide cathode occur in order to improve the repeatibility of the process. Other future directions for this work include varying coating thickness, stoichiometery, smoothness, and implantation depth individually in an attempt to correlate these variables with cathode performance and life.

II. MANUFACTURING APPARATUS

This chapter details the experimental arrangement that was employed in this vacuum arc deposition of oxide cathodes. The apparatus consists of four independent systems that work in unison in order to accomplish a repeatable deposition process. These systems include the vacuum chamber (together with its associated pumping and pressure hardware), the plasma gun (responsible for creating the coating), the high voltage, high current electronics (which trigger and supply the plasma current and substrate bias), and the various diagnostics that are employed to characterize the plasma deposition environment.

II.a. Vacuum System

A photograph of the vacuum chamber in which this work was performed is shown in Fig. II.a.1. The chamber is a stainless steel, cylindrical vessel approximately 66 cm internal diameter by 27 cm internal height for a total chamber volume of approximately 100 liters (if one includes the additional volume of the ports and their tubulation). A variety of Conflat-type flanges surround the side of the vessel, and additional ports of similar type are attached to flanges on the bottom and on the removable lid. Dr. Ian Brown, a colleague at Lawrence Berkeley National Laboratory (see Sect. II.b.), has extensive experience performing vacuum arc deposition in a chamber with a base pressure in the mid 10^{-6} Torr range. In an attempt to improve the cleanliness and

repeatibility of the process, the vacuum system for the current work was designed to operate at or below the mid 10^{-7} Torr scale.

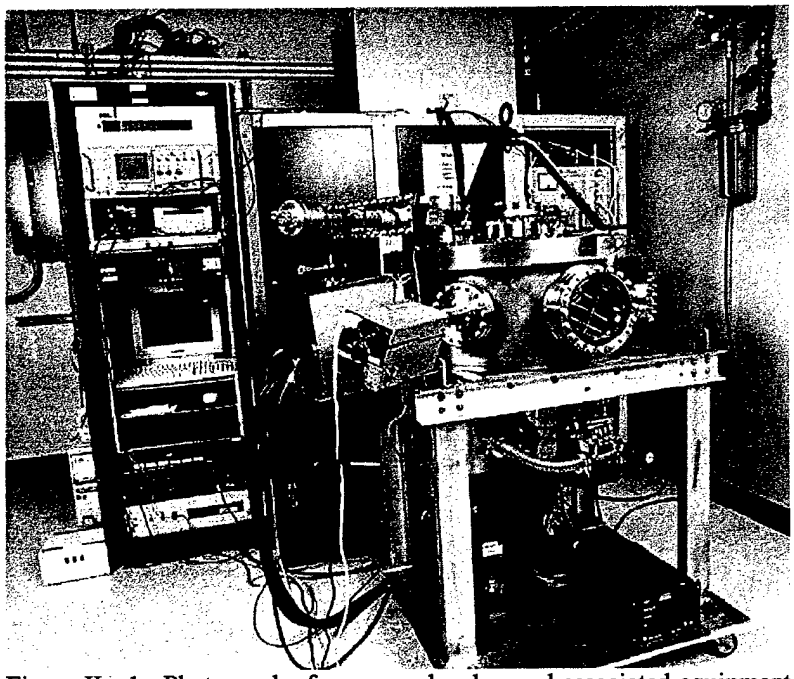

Figure II.a.1. Photograph of vacuum chamber and associated equipment for vacuum arc deposition of oxide cathodes.

Many years ago, this chamber was used for studies of ultra-violet photoemission from virgin metal surfaces in ultra-high vacuum. The chamber used an electro-ion pump to achieve this pressure range, and the lid sealed via a scaled-up Conflat design (opposing knife edges on the chamber lip and lid sealed by biting into a large copper annular gasket). The development of the process for vacuum arc deposition of oxide cathodes required convenient and repeated access to the inside of the chamber, so this knife edge seal was replaced with a more cost- and time-efficient Viton o-ring seal. The o-ring sits in a groove machined into the chamber lip, and the weight of the lid alone is enough to

provide a vacuum seal without the addition of any tightening bolts. The o-ring may soon be replaced with a metal seal on a trial basis to invesitage the possible improvements in base pressure and pumping speed. All other seals on the chamber are Conflat-type with copper gaskets (except where Viton gaskets were used in valves and on ports where limited access prevented full tightening of the required fine thread bolts).

The chamber is pumped by a Leybold Turbovac TMP360V turbopump backed by an Alcatel 2015 two-stage rotary vane roughing pump. The 400 liters per second (N2) turbopump has a 160CF (6" O.D.) high vacuum flange and a 25KF foreline connection; it was retro-fitted with ceramic bearings for oil-free operation. The 298 liters per minute roughing pump was prepared for service in an oxygen environment by using Fomblin lubricant in place of standard oil. The roughing pump has a base pressure of a few milliTorr, which is more than sufficient for maintaining the 100 mTorr maximum foreline pressure required for turbopump operation. A foreline trap and a molecular sieve are placed between the roughing pump and the turbopump in order to help prevent any Fomblin from backstreaming into the vacuum chamber (the roughing pump is also fitted with an automatic valve that closes in order to prevent backstreaming in case of power failure).

Most gases were readily pumped by the turbo, but it was found that water vapor was much more tenacious. Since water vapor is the main poisoning agent for oxide cathodes[1] (barium oxide quickly becomes barium hydroxide and then other various hydrates in the presence of water vapor), it must be removed as quickly as possible. An attempt was made to improve the water vapor pumping speed by adding a cold trap to the

chamber (a sorption pump cooled with liquid nitrogen), but no significant improvement was seen at water vapor partial pressures below 1 x 10^{-5} Torr. The dry nitrogen used to purge the chamber was then heated so that it would help keep the chamber walls warm (to lessen the amount of water vapor adsorption). This warm nitrogen purge was also used during pump down to help jar loose any adsorbed water vapor; the purge was turned on when the roughing pump brought the chamber pressure below 700 Torr, and it was turned off when the chamber pressure dropped below 150 Torr. No significant gain was seen in the water vapor pumping speed. As a last resort, the water vapor may be absorbed by releasing free barium and/or strontium into the chamber by triggering the plasma gun. It was found that 100 shots of the barium/strontium plasma released sufficient free barium and strontium to bring the water vapor partial pressure from the high 10^{-8} Torr scale down to the high 10^{-10} Torr scale. This gettering process was essential for the optimum performance of the coated oxide cathodes.

Pressure in the foreline is monitored using a heat convection gauge, while the pressure in the chamber is monitored using both a convection gauge and a Bayard-Alpert ionization gauge tube. The ionization gauge tube contains a single thoria coated iridium filament. A Granville-Phillips 303 vacuum process controller monitors and displays the pressures sensed by these gauges (the controller also features auto-on and auto-off for the ionization guage to prevent excessive shortening of filament life due to overpressurization).

Optimal base pressure achieved with the chamber and pumping system is below 3 x 10^{-8} Torr. Operation in the low 10^{-8} Torr scale requires the chamber to be warmed up

in order to accelerate pumping of the various adsorbed gases (especially water vapor). Maximum bake out temperature is limited to below 100°C due to the electrical equipment mounted on the chamber. Without baking, the chamber can still be pumped into the mid to high 10^{-8} Torr scale given enough time (typically, three days). Standard operating pressure for the deposition done here was in the mid 10^{-7} Torr range (which can be reached after several hours of pumping). A high 10^{-6} Torr scale vacuum can be achieved within twenty minutes for rapid turn-around testing. The roughing pump takes approximately four minutes to bring the chamber pressure down from atmospheric to about 100 mTorr (when the turbopump is activated). The turbo spins up to speed within two minutes, by which time the chamber is well into the mid 10^{-5} Torr range.

When the system must be opened up, it is vented to atmospheric pressure by filling with warm dry nitrogen (blow-off from a large liquid nitrogen tank which is then piped through a "hot box" for heating). When changing a Conflat flange, nitrogen is left flowing through the chamber in order to minimize the amount of laboratory air entering the chamber. When the entire lid is removed, flowing this small amount of nitrogen is abandoned as futile.

II.b. Plasma Gun

In July of 1996 at the XVIIth International Symposium on Discharges and Electrical Insulation in Vacuum, a minicourse was held on Materials Modification and Thin Film Deposition by Cathodic Arc Methods. It was this course that introduced the

UCD/SLAC oxide cathode team to Dr. Ian Brown of Lawrence Berkeley National Laboratory (LBNL). Based upon preliminary discussions with Dr. Brown, there appeared to be no fatal flaws in applying cathodic arc deposition for laying down barium and strontium oxides onto a nickel base thereby making an oxide cathode.

Dr. Brown had worked on ion sources[2] for many years, which then led to his work on metal plasma immersion ion implantation and deposition.[3] The plasma gun developed by Dr. Brown at LBNL[4] chosen for this vacuum arc deposition process is shown in Fig. II.b.1.

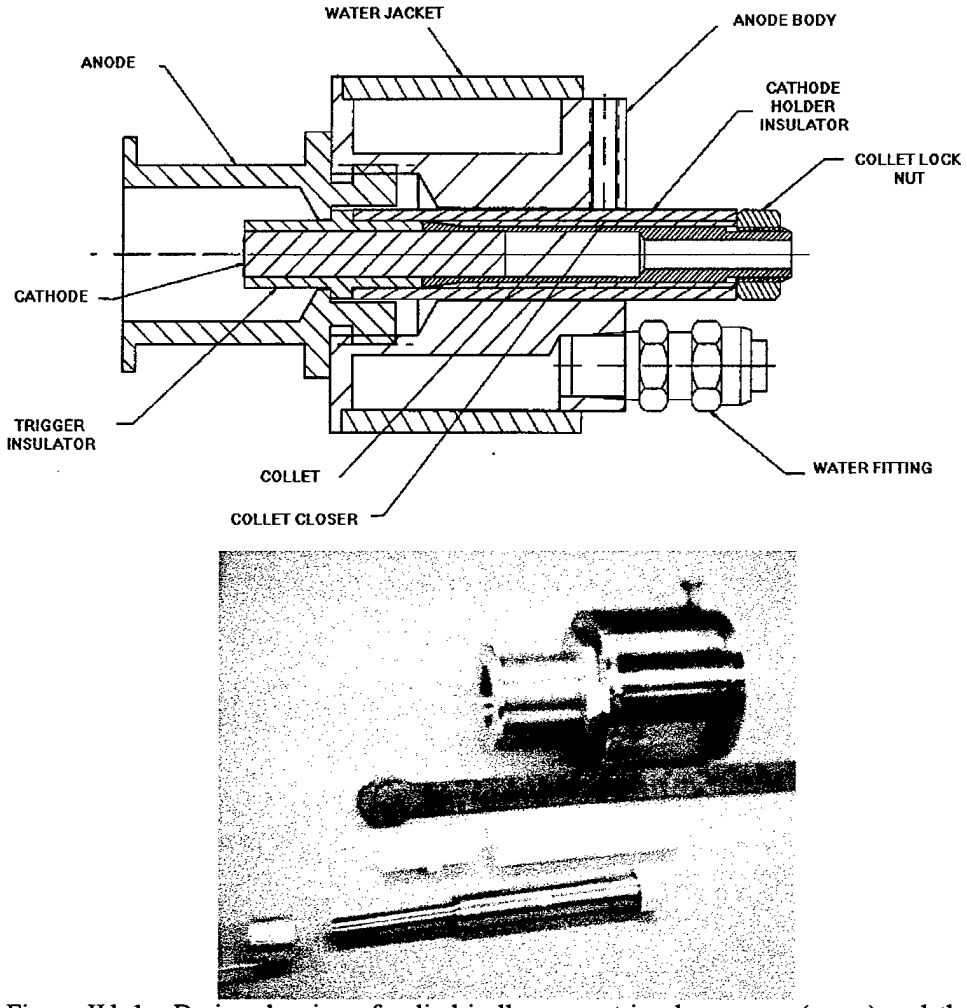

Figure II.b.1. Design drawing of cylindrically symmetric plasma gun (upper) and the partially disassembled completed gun (lower). Shown in the photo are the anode (top), insulating ceramics (middle), and cathode with trigger cap (bottom).

With this plasma gun geometry, the plasma is initiated by applying a positive high voltage trigger pulse to the trigger cap which causes an arc to develop between the trigger cap and the grounded cathode (i.e. the plasma source; a certain amount of unavoidable confusion arises due to the plasma source being labeled a cathode while the target of the deposition is also labeled a cathode. It should remain clear from context which cathode is being referenced). The energy of this arc is sufficient to ionize some of the cathode

material thereby filling the cylindrical anode cavity with plasma. Prior to cessation of the short (microseconds) trigger pulse, a longer (milliseconds), lower voltage positive pulse is applied to the anode. This second pulse then maintains the arc between the cathode and anode thereby generating copious amounts of plasma from the cathode material. The pressure of the plasma at the source causes a rapid and violent expansion of the metal plasma away from the source and out the anode. Some of the plasma is intercepted by the anode thus completing the cathode-to-anode circuit for the current flow, but much of the plasma is ejected out from the gun and is available to be deposited on the first surface it touches.

Additional details on vacuum arc deposition are exhaustively covered in the 1994 compilation **Handbook of Vacuum Arc Science and Technology**;[5] therfore, only a brief description of pertinent features is given here as summarized in February of 1998 by R. A. MacGill, et al.[6] The vacuum arc generates copious amounts of metal plasma that is highly ionized with charge state components of typically 2+ or 3+ but sometimes up to 6+ (depending on cathode material). The plasma is actually generated at a finite number of micron-size regions on the cathode surface known as cathode spots. These intensely heated regions spontaneously ignite and extinguish during the plasma pulse as they move across the cathode surface. A minimum current on the order of tens of amperes is necessary to keep a spot from extinguishing immediately, and boosting the total current increases the number of cathode spots at any given time thereby holding the current per cathode spot relatively constant. The plasma plumes away from the spot with a directed ion velocity on the order of 1-2 cm/μs independent of cathode material. The actual

thermal velocity of the ions is only roughly one tenth of the component normal to the cathode surface. The energy at which the ions impinge upon the substrate may be tailored by applying a pulsed negative bias that accelerates ions into the substrate (the bias must be pulsed in order to prevent arcing from the plasma to the substrate). With sufficient bias amplitude, ions may be implanted into the substrate during the pulse while deposition on the substrate surface continues during the unbiased phase. Such bias was found to improve both the smoothness and adhesion properties of vacuum arc deposited films.

Rapid expansion of the plasma as it leaves the cathode tends to distribute the plasma into a wide cone that deposits onto any line-of-sight surface. In order to increase the efficiency of the deposition, one needs to focus the plasma into a somewhat narrower beam. Several turns of current-carrying wire are wound around the cylindrical anode. The magnetic field lines thus created have the added benefit of slowing the migration of the charged particle-filled cathode spots (if a cathode spot reaches the edge of the cathode face, it extinguishes). The current can be most simply supplied by passing the main plasma arc current through the coil (the windings are then in series with the rest of the arc circuit). Additional focusing may be provided by implementing a guiding coil for the plasma as described in the next paragraph.

Along with the spectrum of multiply charged ions, the cathode spots also emit some neutral gas as well as solid debris known as "macroparticles." These macroparticles, initially molten but rapidly cooled to a solid state, are roughly 0.1 to 10 microns in diameter. The number of macroparticles generated differs with cathode

material (fewer particles for higher melting point metals). Macroparticles are preferentially emitted nearly parallel to the cathode surface as opposed to the normal trajectory of the ionized plasma plume. Nevertheless, macroparticles do find their way to the substrate, thereby degrading the smoothness of the vacuum arc deposition film. Typically, these macroparticles are removed from the deposition plasma by using a current-carrying coil to magnetically guide only the charged particles toward the substrate. Such schemes have been extremely successful in removing macroparticles from the deposited film in exchange for a lower deposition rate (some of the plasma is lost to the coils of the filter). In the current work, no macroparticle filter was used in order to maintain a higher deposition rate. Removal of the macroparticles was not considered critical at this stage since the presence of macroparticles would not degrade the emission density of the oxide cathode thus created. In future work, if it is found that the macroparticles reduce the oxide cathode electron beam quality by distorting the fields on the surface, then the macroparticles must be removed via a magnetic filter as described above. Such removal of the macroparticles will also improve the repeatibility of the cathode deposition process which may thereby improve cathode reliability and/or lifetime. Larger substrates may be coated as well by moving the substrate in vacuum so that an even coating may be deposited. A schematic of such a layout is shown in Fig. II.b.2.

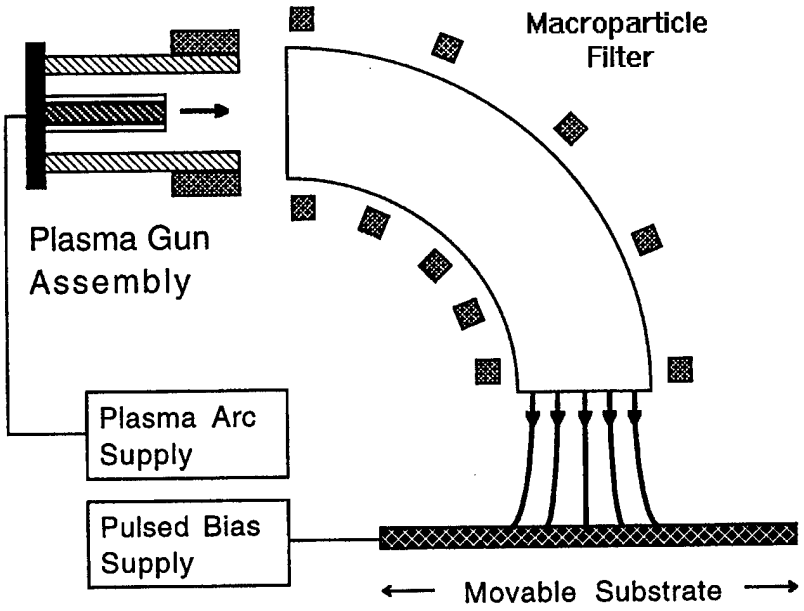

Figure II.b.2. Setup for plasma gun, macroparticle filter, and movable substrate

By far, the most difficult aspect of applying vacuum arc technology for the deposition of oxide cathodes was the lack of a reliable, repeatable trigger for the plasma pulses. Initial tests of barium deposition were done in Dr. Ian Brown's laboratory at LBNL. The highly reactive barium cathode rods oxidized so quickly in air that their electrical connections were extremely unreliable. This problem was later overcome by using nickel sleeves that had been filled with barium (electrical connection was made to the nickel sleeve in contact with the barium; only the barium at the ends of the rods could now oxidize). In Dr. Brown's plasma gun configuration, the plasma is initiated via ions evaporated from the surface of a resistive thin film. The ceramic insulator that holds off the voltage from the cathode to the anode is covered with a resistive thin graphite film. When the trigger pulse is placed across the cathode and anode, current flow through the film generates enough heat to evaporate and even ionize small amounts of the carbon.

The presence of these ions in the anode cavity provides the current path necessary to initiate cathode spots which are then maintained by the metal plasma. Carbon evaporates off in the triggering phase, but some cathode material is deposited back on to the ceramic during the main arc pulse. As long as the film continues to evaporate sufficient material to initiate the discharge, then successful triggering can be maintained. Unfortunately, carbon would poison oxide cathodes, so experiments with alternative thin films were conducted. Nickel and molybdenum thin films were used, but it was found that the coating resistance varied greatly from shot to shot so that film evaporation was never guaranteed. Rather than rely on a thin film whose properties changed rapidly, the trigger scheme was changed to a spark gap configuration. In the current work, a small trigger cap (either aluminum or tungsten; both are compatible with oxide cathodes) is inserted over the ceramic insulator after the cathode is docked into the anode (see Fig. II.b.1.). The cap is machined to leave a 25 mil radius gap from the cathode rod to the trigger cap along the ceramic insulator surface. With sufficient voltage difference (several kilovolts), breakdown is consistently accomplished followed by a successful trigger pulse that creates sufficient charged particles to begin the cathode to anode discharge. The drawback of this scheme is that cathode material slowly builds up in the gap from the cathode to the trigger cap. Thus, once sufficient conductive film has bridged the cathode-trigger gap, the two are shorted together and the plasma no longer triggers successfully. A variety of trigger-cap-to-cathode-rod gaps were tried (from 5 to 35 mil radius gap), but the most reliable triggering occurred with a 25 mil radius gap. With this triggering scheme, a few thousand plasma shots can be fired before having to clean/recondition the

ceramic insulator. Typically, one thousand shots were used to deposit the oxide film on the nickel substrate, so this scheme was adequate. To improve the longevity of the trigger circuit, one possibility is to redesign the gun such that the trigger cap lies below the plane of the cathode surface so that it is much more difficult for a film to develop a complete connection from cathode to trigger cap. Eventually, a laser triggering scheme may be implemented whereby a moderate power laser pulse evaporates and ionizes sufficient cathode material such that the cathode-to-anode discharge may begin.

As mentioned above, the cathode rods used in the present work are actually nickel tubing filled with barium or a 50% atomic barium/strontium mix (it was found that the atomic deposition rates for barium-filled tubing and strontium-filled tubing were roughly the same, so to achieve an approximately 50:50 barium to strontium ratio in the oxide coating, one need only generate the deposition plasma from a 50:50 mixed source). The nominal wall thickness of the tubing is 20 mils. Molten barium or barium/strontium is then sucked into the tubing. Rods were received packaged in mineral oil to prevent oxidation of the barium and strontium. Before loading a rod into the vacuum chamber, the rod was cleaned with mineral spirits (acetone and ethanol are incompatible with barium and strontium), and the emission end of the rod was faced off on a belt sander to expose fresh metal. It was found that the barium and strontium triggered reliably and that they both eroded much more quickly than the surrounding nickel tubing.

II.c. Electronics

Described in this section are the electronics used to generate the plasma, maintain the plasma arc, and provide a bias to the substrate in order to encourage implantation as well as deposition. A schematic diagram of the unified system is shown in Fig. II.c.1 and is described in detail below.

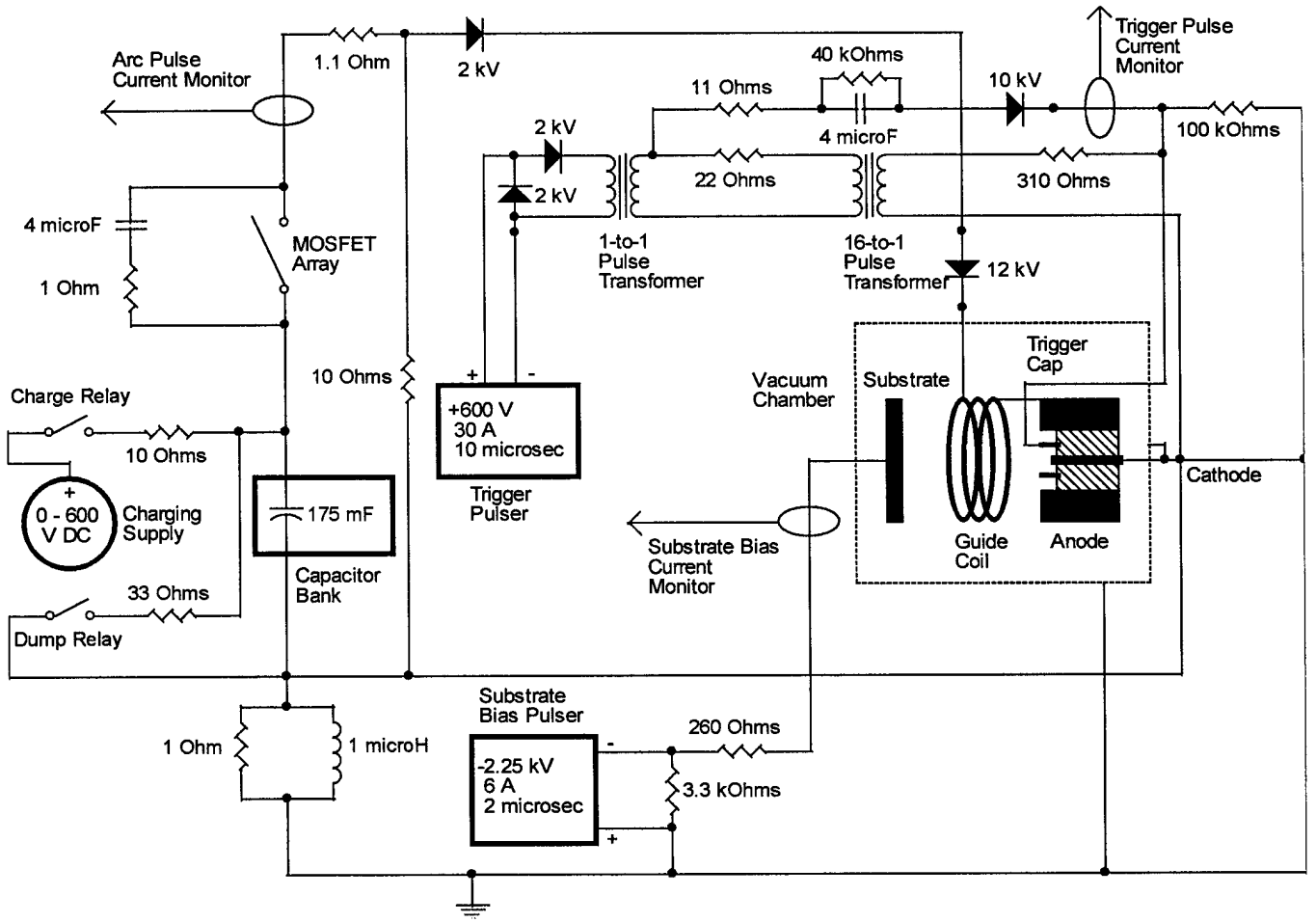

Figure II.c.1 Vacuum arc deposition electronics.

The plasma is operated in a pulsed DC mode. The main plasma discharge is typically 130 A for 12 msec, and it is run at a repitition rate of 1 Hz (1.2% duty). The discharge is initiated via a short duration (several microseconds) high voltage pre-pulse which is also run at 1 Hz. During the discharge, the substrate bias is gated on for 2 μsec intervals before being gated off for 10 μsec (thus resulting in a 17% duty factor, but only during the 12 msec main plasma pulse). This gating allows deposition and implantation to occur in rapid succession as the film thickness begins to build. Sequencing of these pulses is controlled via a Stanford Research Systems DG535 four channel digital delay/pulse generator.

The initial spark which generates plasma inside the vacuum chamber begins as a short duration (~ 10 μsec), medium voltage (~ 600 V) pulse produced by a Velonex 360 high power pulse generator. A model #1767 plug-in unit is used in this Velonex in order to provide an appropriate voltage and current level from the pulser; several amperes of current are necessary to maintain a vacuum arc cathode spot. Such high current cannot be provided by the higher voltage plug-ins available for this pulser. The pulse travels through five meters of high voltage coaxial cable (Belden 8267) before entering the high voltage electronics box that is attached to the vacuum chamber. Inside this box, the Velonex pulse passes through 2 kV steering diodes before entering a 1-to-1 ratio pulse transformer. The steering diodes and pulse transformer are employed primarily to protect the Velonex from "seeing" the main capacitor bank discharge that feeds the plasma after triggering. The output of the transformer is then split into two separate paths.

The first path is through current-limiting resistors to a 16-to-1 ratio step up transformer. This transformer steps the Velonex pulse up into the kilovolt range (10 kV maximum) for just a few microseconds before the transformer saturates. This voltage spike causes a vacuum arc discharge to occur between the grounded cathode and the trigger cap of the plasma gun which is mounted nearby (described in Sec. II.b. above; see Fig. II.b.1.). The discharge is very low impedance (less than one ohm), and the plasma generated quickly fills the anode cavity. Thus, the discharge is free to continue through the low impedance path of cathode-to-anode after the cathode-to-trigger-piece pulse is discontinued.

The second path for the Velonex pulse out of the 1-to-1 transformer is through a current-limiting series RC circuit. In conjunction with the short duration high voltage pulse, several amperes of current must be available to continue the discharge while still providing a nonzero voltage to the anode. This leg of the trigger circuit provides up to 50 A of current that may be drawn during the 10 μsec trigger pulse after the initial breakdown. Typically, 30 A were drawn during a trigger pulse.

In order to prevent the rest of the electronics from seeing the several kilovolt trigger pulse, protection diodes are used in key places. The 600 V leg of the trigger circuit is protected by a small 10 kV, 500 mA average forward current diode. The main capacitor bank is protected by a 12 kV stack of hockey puck diodes which are used because of their high forward current-carrying capability. In the event of an unsuccessful trigger (no plasma breakdown), a 100 kΩ path is provided from high voltage to ground in order to subdue any charge build up (RC time constant is 400 msec).

The trigger pulse is placed across the trigger cap and cathode of the plasma gun in order to achieve a fast breakdown. Once the breakdown has occurred, it is up to the main capacitor bank to supply the necessary voltage and current to maintain the metal plasma. The capacitor bank used for this system was originally built to supply current to magnet coils as part of Dr. William J. Corbett's Master's thesis.[7] These coils were used to produce the magnetic field for a set of toroidal cusp plasma experiments in the late 1980's at the University of California, Los Angeles. The capacitor bank uses two hundred 3500 μF, 450 V electrolytic capacitors; two segments of 100 parallel capacitors are in series to provide a total of 175 mF with a maximum charging voltage of 900 V. Each capacitor has one of its terminals wired through a #26 gauge lead to serve as a fuse. The bank is charged using three phase 208V AC power which is run through a variac to a step-up up transformer before being rectified by a three phase full wave rectifier. Maximum charging output is 10 A at 740 V DC.

The capacitor bank was originally switched using an ignitron to start the discharge which then continued until the capacitors had fully discharged. For the pulsed DC operation required here, a switch was needed that would not only switch on the bank but also switch it off. Dr. Hugh Kirbie of Lawrence Livermore National Laboratory was kind enough to provide a parallel array of 12 solid state MOSFET's in order to do this job. Each FET holds off up to 1 kV and can pass 50 A in a pulsed mode. The array is mounted on a printed circuit board powered by 24 V DC and triggered via an optical pulse. An RC snubber is connected across the board in order to dampen voltage spikes that may occur when hundreds of amperes are switched off and on with short rise/fall

times. Directly on top of the rack that holds the capacitor bank and MOSFET array are mounted the current-limiting resistors. Nine noninductive, 1 kW resistors were used in parallel to achieve the 1 Ω path from the capacitor bank to the vacuum chamber. A single 10 Ω resistor was used as a shunt to ground in order to provide a current path in the event of an unsuccessful trigger pulse. A 2 kV protection diode array is connected immediately following the resistors in order to help protect the FET array from any voltages induced at the vacuum chamber or any voltage leakage through the 12 kV hockey puck diode stack at the chamber.

The main plasma current provided by the capacitor bank flows first into the guide coil of the gun before passing to the anode and then to the grounded cathode. The current flowing through the coil helps confine the plasma as it ejects from the cathode surface toward the substrate. The capacitor bank is set to trigger 2 μsec after the 10 μsec Velonex trigger pulse begins so that there is sufficient overlap between the two pulses. Breakdown typically occurs within a microsecond, after which the Velonex continues to supply the necessary current until the capacitor bank begins dumping current in as well. By the time the Velonex pulse terminates, the capacitor bank is sustaining the arc with several tens of amperes of current.

The main arc current rapidly (several microseconds) builds up to its peak (typically run with the capacitor bank charged to 200 V to supply roughly 140 A of current). During this discharge, a Velonex 350 high power pulse generator is gated off and on in order to supply a substrate biasing voltage. A model #1097 plug-in is used in order to generate a short duration, low current, -2.25 kV pulse. A 260 Ω resistor limits

the current drawn from the plasma to roughly 8 A, and a 3.3 kΩ parallel resistor provides a load for pulses when there is no plasma at the substrate. This –2.25 kV bias is gated on for 2 μsec and then off for 10 μsec. The "on" duration is kept short so that arcing between the plasma and the substrate does not have time to occur. After approximately two hundred angstroms of coating have been deposited, the –2.25 kV is reduced to just –400 V so that the accelerated ions no longer implant themselves deeply and sputter off some of the coating in the process. The high voltage is only required in the beginning stages of the deposition/implantation so that the implanted ions can bury themselves on the order of a hundred angstroms into the substrate while sputtering off substrate material[8] (the actual implantation depth is dependent upon both substrate and target materials as well as the negative bias pulse). After the coating thickness is larger than the implantation depth, continuing to apply a high voltage bias would only implant the coating into the coating rather than into the substrate with the additional detrimental effect of sputtering off some of the coating in the process.

II.d. Diagnostics

In order to characterize and ensure the repeatibility of this deposition process, several diagnostics are employed. By far, the most valuable tool has proven to be the residual gas analyzer for identifying the individual components of the background gas in the chamber. Other useful process diagnostics include a rate thickness monitor for determining deposited film thicknesses, an optical emission spectrometer for rough

determination of plasma constituents based upon characteristic excited emission lines, and a translatable electrostatic Langmuir plasma probe for determining plasma densities and temperatures at various locations. In addition, pulsed current transformers and a fast high voltage probe were used to measure other process variables such as the vacuum arc trigger voltage and current, the main plasma pulse current, and the substrate bias voltage and current.

Pulsed currents in this experiment were all measured using Pearson pulse current transformers. The main arc current was measured with Pearson model 301X (0.01 V/A output), the trigger current with model 110A (0.1 V/A output), and the substrate bias current with model 2100 (1.0 V/A output). Pulsed voltages were measured using a single Tektronix fast high voltage oscilloscope probe. The Tektronix P6015A probe is a 1000-to-1, 3.0 pF, 100 MΩ probe rated for pulses up to 40 kV with 100 msec max duration.

Shown in Fig. II.d.1 are the initial plasma parameters during a typical successful pulse. Breakdown of the vacuum arc occurred within the first microsecond near 6.6 kV which coincided with the rise of the trigger current to roughly 30 A. Two microseconds after the trigger pulse is begun, the main arc current is turned on and rises to its peak value of 130 A within 35 μsec. The trigger voltage is turned off after 10 μsec, at which point a slight current reversal occurs (a capacitive discharge limited by reversed-biased diodes) which dissipates within 4 μsec. A small amount of current may flow from the anode to the trigger cap if the trigger cap bias turns slightly negative with respect to the grounded cathode; this effect may be seen in the slight dip of the main arc current about

14 μsec into the pulse. This main arc pulse contiues for 12 msec (nearly flat-top) at which time it is shut off (fall time is approximately a few microseconds).

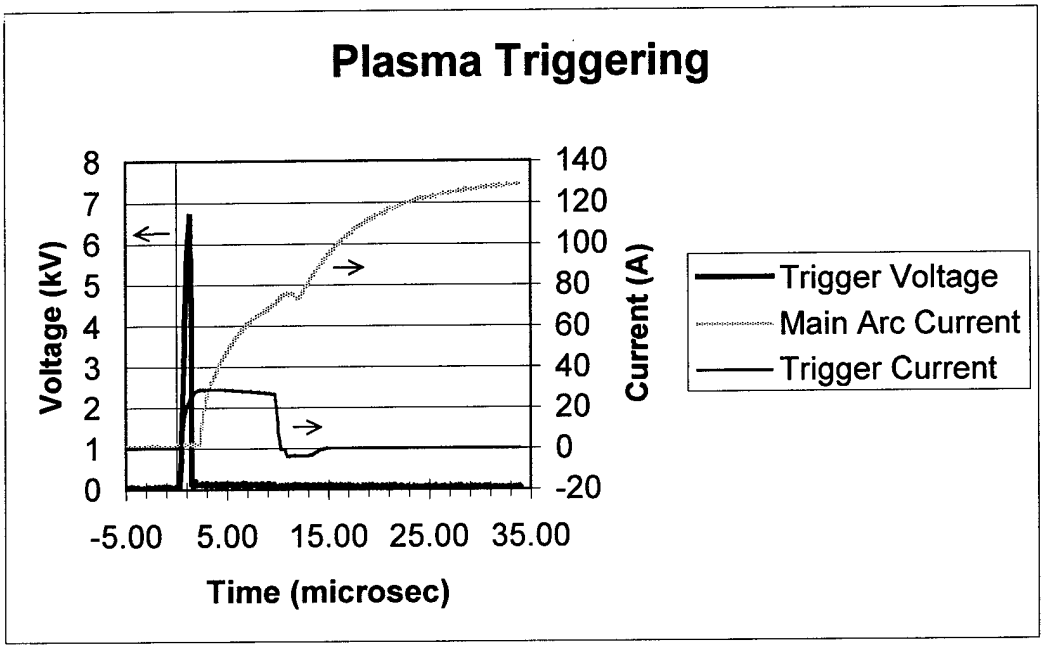

Figure II.d.1. Initial plasma parameters as measured by pulsed current transformers and a fast high voltage probe during a typical successful plasma pulse.

During the 12 msec duration plasma pulse, the substrate is continually pulsed at high negative voltage to encourage ion implantation. Typically, a 2.25 kV pulse is used during the first couple of hundred of angstroms of coating, after which the biased is reduced to 400 V. The voltage at the substrate and the current drawn from the substrate are shown in Fig. II.d.2.

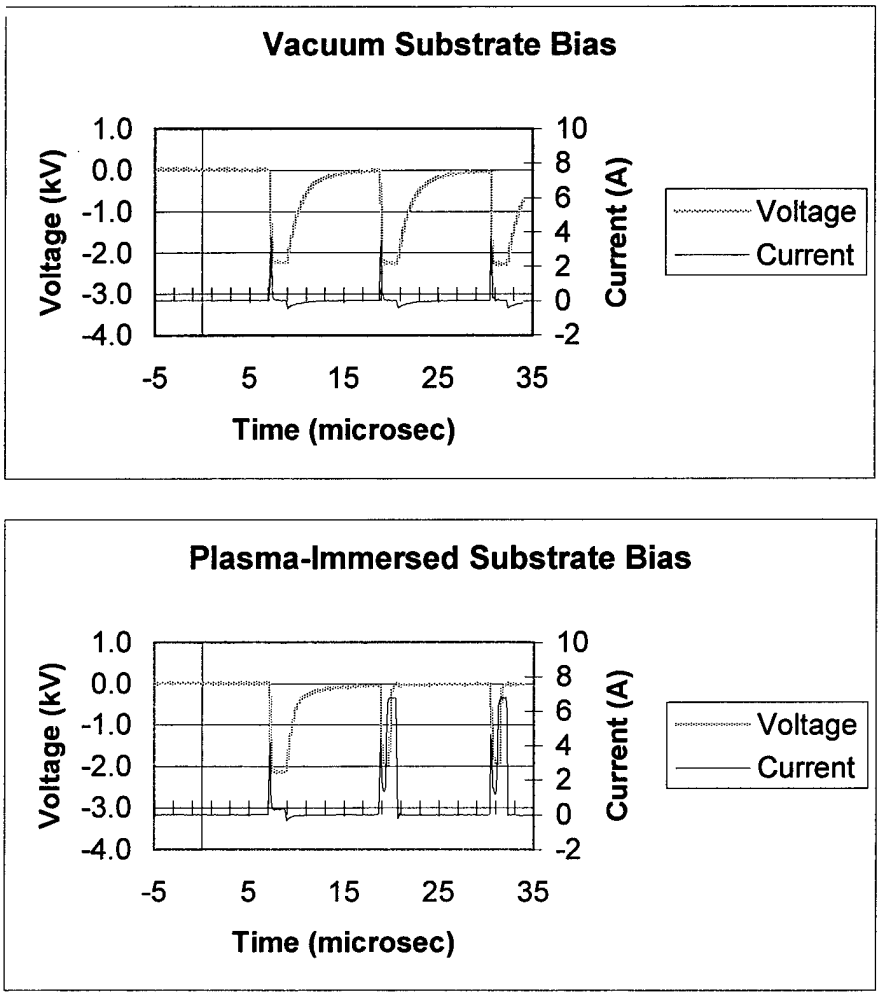

Figure II.d.2. Voltage and current traces for the substrate bias in the absence of plasma (top) and in the presence of plasma (bottom).

When there is no plasma present, the voltage trace clearly shows a flat 2 μsec duration – 2.25 kV pulse which discharges to an off state for 10 μsec before beginning the pulse sequence again. A brief capacitive charging current is drawn at the beginning of each pulse, but it rapidly decays away; a longer duration discharging current is also visible on the current trace. In the presence of the 12 msec plasma pulse, the voltage at the substrate can no longer be held at –2.25 kV during the 2 μsec pulse. The plasma serves as a nearly infinite source of current at a potential nearly zero relative to the –2.25 kV

pulse, so the voltage of the pulse is dropped across the current limiting resistors in series with the pulse. Again, the current trace begins with a brief capacitive charging spike, but rapidly flattens out to 6.8 A of current during the 2 μsec pulse. The maximum current is regulated by the aforementioned current-limiting resistors. To further examine the effect the presence of the plasma has on the substrate bias voltage and current, another set of traces are shown in Fig. II.d.3.

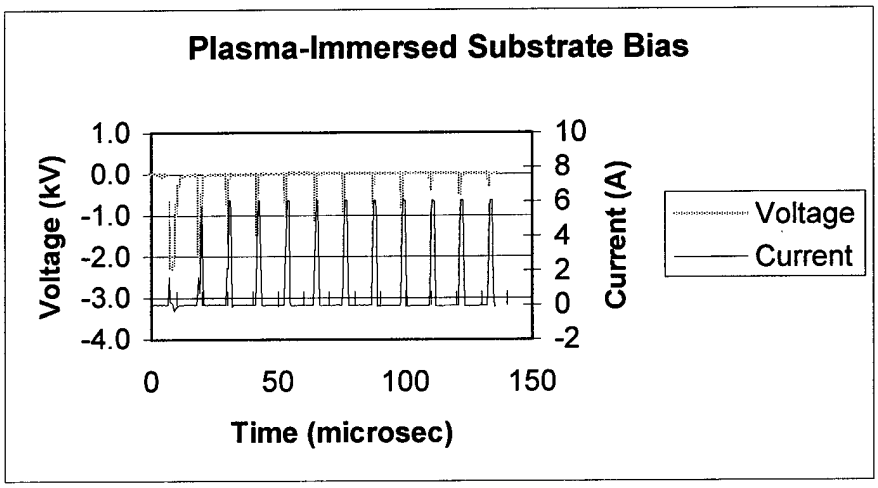

Figure II.d.3. Longer time scale voltage and current traces for the substrate bias in the presence of plasma.

On this longer time scale, it becomes clear that the capacitive charging current disappears relative to the current drawn from the plasma, while the voltage at the substrate decays with each successive pulse. During the remainder of the 12 msec plasma pulse, the substrate continues to draw 6 A of current during each 2 μsec bias pulse from the near-zero potential plasma. After 200 plasma shots, the bias voltage is reduced to 400 V with similar voltage and current traces.

To estimate the plasma potential as well as other important plasma parameters, a movable electrostatic plasma probe was introduced into the plasma. The Hiden Analytical Electrostatic Plasma probe (ESP) system includes a tungsten probe tip (4.7 mm^2 area) mounted on an insulating rod attached to a linear drive capable of 12" of travel. A rack-mounted controller and separate amplifier (for high current operation up to 1.0 A) are attached to the probe as well as to the computer which controls the probe via Hiden's interface software and a standard RS232 serial port link. The probe tip is gradually introduced into the plasma by 1.0 cm steps (the length of the tip is 1.0 cm, so the tip automatically supplies an average over that 1.0 cm of the plasma parameters). At each position, the probe tip is biased from a negative voltage (typically –40 V) to a positive voltage (70 V) in steps of one volt. At each step, the current drawn to the tip is measured. Analysis of a typical set of current versus voltage traces is postponed until Chap. IV, Results & Discussion, so only a few brief comments are made here. From each trace, one can estimate the plasma potential, the electron energy, the electron and ion densities, and the Debye length of the plasma at each probe tip position. Since the plasma is pulsed on for only 12 msec at 1 Hz, the data are also taken in a pulsed mode. The probe controller is gated on by the pulse generator used to control all of the plasma electronics so that the probe only takes data in the presence of plasma. During the 12 msec plasma pulse, a 10 msec control pulse is sent to the probe to allow it to take data (the first and last millisecond of the plasma pulse are cut out). At each voltage setting, the probe is allowed to settle for 30 msec (roughly three plasma shots) before reading the current during a single 10 msec window (one plasma shot). Then, the voltage is stepped

up and the process is repeated. The very brief window for taking the current data holds some responisibility for the noise level of the data. Of course, since the data requires many plasma pulses for a complete I-V curve, the shot-to-shot repeatability of the plasma is also a noise issue. Nevertheless, fitting analyses on the traces yield approximate plasma parameters and are presented in Chap. IV.

Another tool for diagnosing the deposition plasma is the optical emission spectrometer (OES). This diagnostic collects light emitted from the pulsed plasma and displays intensity versus frequency. These emission lines are then compared to known excitation lines in order to determine the gross composition of the plasma. The Ocean Optics spectrometer is fitted with three separate gratings, each calibrated for a specific wavelength region. The master channel accepts light between 150 nm and 1350 nm but with poor resolution, while the first slave narrows in on the 200 nm to 520 nm region and the second slave functions from 400 nm to 700 nm. A quartz window (which transmits UV light better than standard glass) is mounted on a 2.75" Conflat flange that has a view of the light emitted by the plasma. A UV-rated fiber optic cable with a wide field of view lens collects the light and transmits it directly to each of the three spectrometer channels (the cable is trifurcated at one end to allow for sending the light to all three channels at once). Like the electrostatic Langmuir plasma probe, the spectrometer is computer controlled and can be gated on by the pulse generator only during plasma events. It was found that the 10 msec window did not produce sufficient light in all of the channels for a well-resolved signal, so a longer collection/integration time was used. Each channel collects light for a total of 2200 msec (two plasma shots) before processing the data and

displaying it. Before the plasma pulsing is started, a background spectrum is taken for each spectrometer channel. Then, this background spectrum is subtracted from future spectra. Thus, every few seconds the spectrometer software updates each of the three channels with spectra averaged over two plasma shots (the software takes a couple of seconds to process each set of data). A typical emission spectrum from a barium/strontium mixed plasma is shown in Fig. II.d.4.

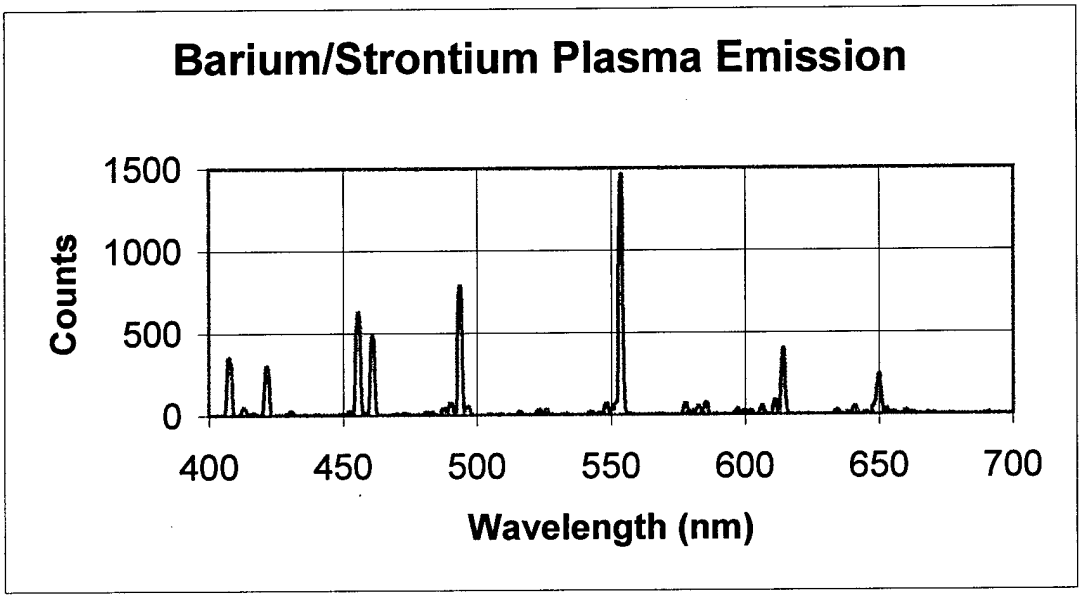

Figure II.d.4. Optical emission spectrum from a vacuum arc plasma consisting of a mixture of barium and strontium.

Again, analysis of the various spectra is reserved for Chap. IV, Results & Discussion, but of the eight prominent lines visible in the spectrum above, five are from neutral and singly ionized barium and three are from neutral and singly ionized strontium (higher levels of ionization were most likely present but not detected due to their extremely low intensities relative to the neutral and singly ionized excitation lines).

Another tool for monitoring the reproducibility of the deposition is the Leybold Inficon XTC/2 rate thickness monitor installed in the vacuum chamber. The unit consists of a rack-mounted controller which electrically connects to the thickness monitor via a 2.75" Conflat feedthrough. On this same feedthrough are compressed air connections (which open and close the shutter for the monitor) and water cooling lines (which may be used to cool the monitor for high deposition rate use where heating of the monitor causes error). The monitor consists of a thin disk-shaped gold crystal mounted on a holder inside the chamber. Since the characteristic frequency at which the crystal prefers to oscillate changes linearly with the mass of the crystal, a measurement of the change in the crystal's natural oscillation frequency can be used to calculate the total amout of mass that has been deposited onto the crystal face. Given the crystal area and the deposition material density, an average coating thickness over the entire crystal surface area may then be approximated with a resolution of one angstrom. An experimental scaling parameter is also introduced to account for differences in the sticking probability of various films as they deposit. The crystal is mounted in a fixed location inside the vacuum chamber where it is exposed to a small amount of the deposition plasma. A tooling factor then needs to be calculated in order to determine the actual coating thickness at the position of the substrate versus the coating thickness on the crystal. This was done by placing a silicon wafer at the location normally used for the oxide cathode nickel buttons inside the chamber. A nickel plasma is then deposited onto the silicon (and the rate thickness monitor crystal). The rate thickness monitor's calculated average thickness is then compared to the measured thickness across a single height profile of the

nickel film on the silicon. The film thickness was measured using a scanning probe microscope (SPM) which required a relatively sharp edge between the deposited film and the substrate. Before mounting in the vacuum chamber, the silicon wafer was marked with a permanent marker; after the nickel deposition, acetone was used to wipe the silicon wafer thereby removing the part of the film that was deposited over the ink. In this manner, a sharp edge was achieved between the nickel film and the silicon wafer. The scanning probe microscopy profiles of two such wafers are shown in Fig. II.d.5.

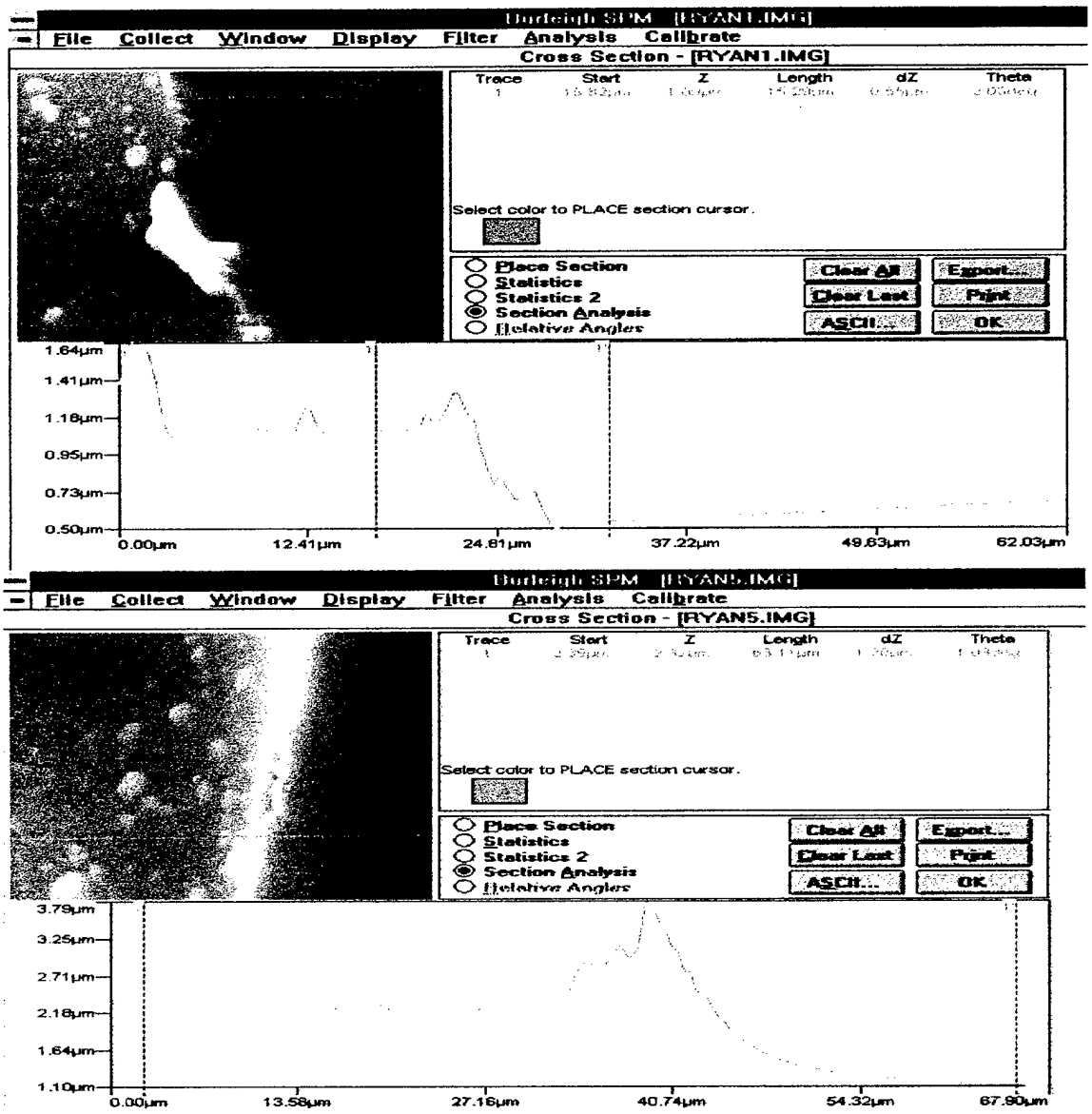

Figure II.d.5. Scanning probe microscopy images and height profiles of two silicon wafers coated with different nickel thicknesses.

For each height profile, a point on the film and a point on the substrate are chosen; the height difference (dZ) between these two points is then calculated. The upper profile shows a measured thickness of 550 nm (SPM) for the wafer coating while the thickness

monitor crystal received 124.4 nm of coating (for a 22.6% tooling factor). The lower profile shows a measured thickness of 1,200 nm (SPM) at the wafer with 337.6 nm at the crystal (for a 28.1% tooling factor). Thus, the coating thickness at the position of the substrate (the oxide cathode) is roughly four times the coating thickness at the rate thickness monitor crystal. This calibration was then used in order to verify the deposition of roughly one to two microns of oxide coating on each of the cathodes made and tested.

The final, and most indispensible, diagnostic used in this deposition process is the Stanford Research Sysems RGA200 residual gas analyzer (RGA). The RGA is mounted on a 2.75" Conflat flange on the deposition chamber. It is controlled via a standard RS232 serial port with the manufacturer's software. The RGA has a filament which ionizes gas atoms before they are accelerated into a quadrupole mass filter where they are counted. The RGA200 is capable of measuring mass-to-charge ratios from 1 to 200 (for the most part, singly ionized atoms are assumed so that the mass-to-charge ratio corresponds to the atomic mass unit number). Since oxide cathodes are extremely sensitive to poisoning by water vapor, it was important to monitor water vapor at each stage of each cathode's life. Additional information was also gained by observing the partial pressures of the other main constituent gases and how they changed throughout the various processes. A typical RGA scan is shown in Fig. II.d.6.

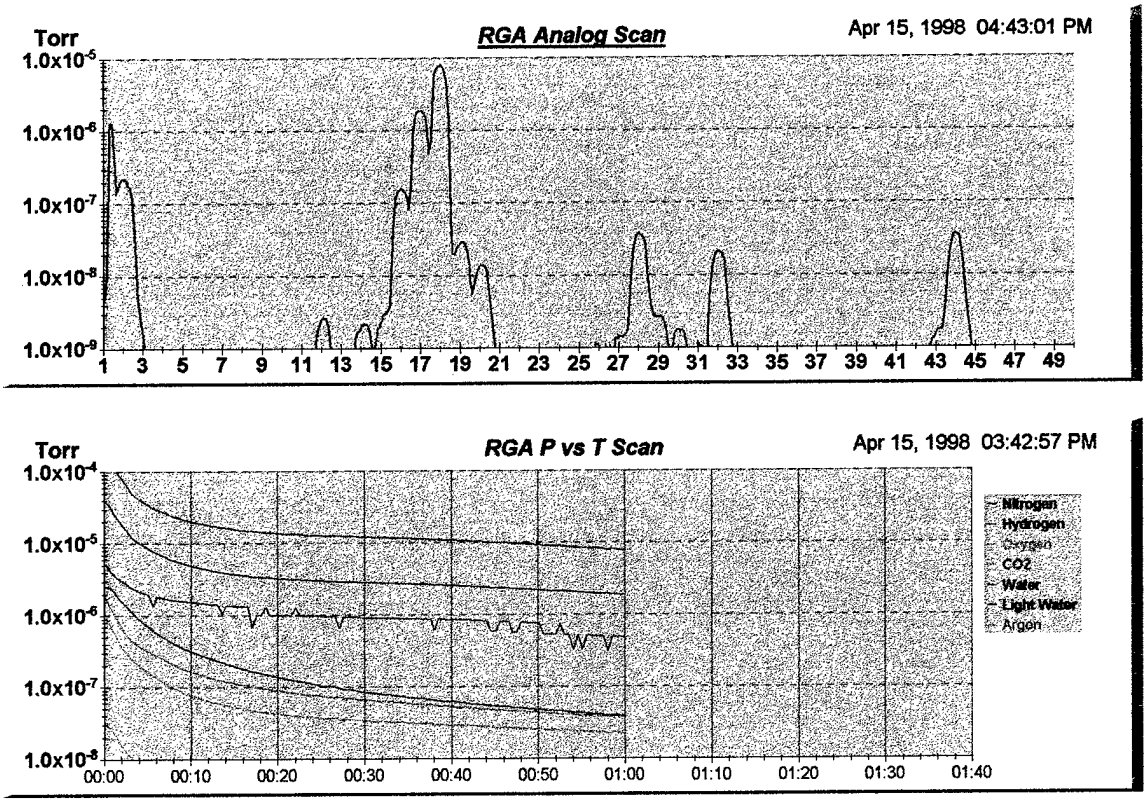

Figure II.d.6. RGA scan from 1 to 50 (top) one hour into a typical pump down tracked over time by a P vs. T chart (bottom).

The main constituent of the background gas is seen to be water vapor (as evidenced by the 16-20 peaks). Hydrogen (2) is also prevelant along with varying amounts of nitrogen (28, 29 and 14), carbon dioxide (44, 28, and 12), and oxygen (32). Residual gas analysis is complicated by the fact that various gases can occupy the same mass-to-charge ratio. In addition, a single gas actually has a distribution of mass-to-charge ratios due to atomic isotopes and occasional double ionization. Nevertheless, RGA data may be used to monitor the repeatibility of the background environment for the deposition process. In addition, the RGA was also used heavily during the activation and testing of the oxide cathodes as is detailed in Chap. IV, Results & Discussion.

The vacuum system, plasma deposition gun, high power electronics, and process diagnostics described above all worked in concert in order to produce a well-characterized process for making oxide cathodes. This same vacuum chamber was then used to test each oxide cathode using the setup described in the next chapter, Analysis Apparatus.

III. ANALYSIS APPARATUS

This chapter describes the cathode packages employed in these experiments together with the methods and equipment used to test the cathodes. For completeness, brief developments of the theory of thermionic cathode emission are also presented so that they may be compared to the actual measured emission characteristics of the present cathodes.

III.a. Oxide Cathode Package

In all of the current experiments, the initial substrate that receives the oxide coating is a cylindrical nickel button that is 3.58 mm in diameter (thus, the area of the cathode is 0.10 cm^2). The button is mounted in a cylindrical cathode package depicted in Fig. III.a.1 below.

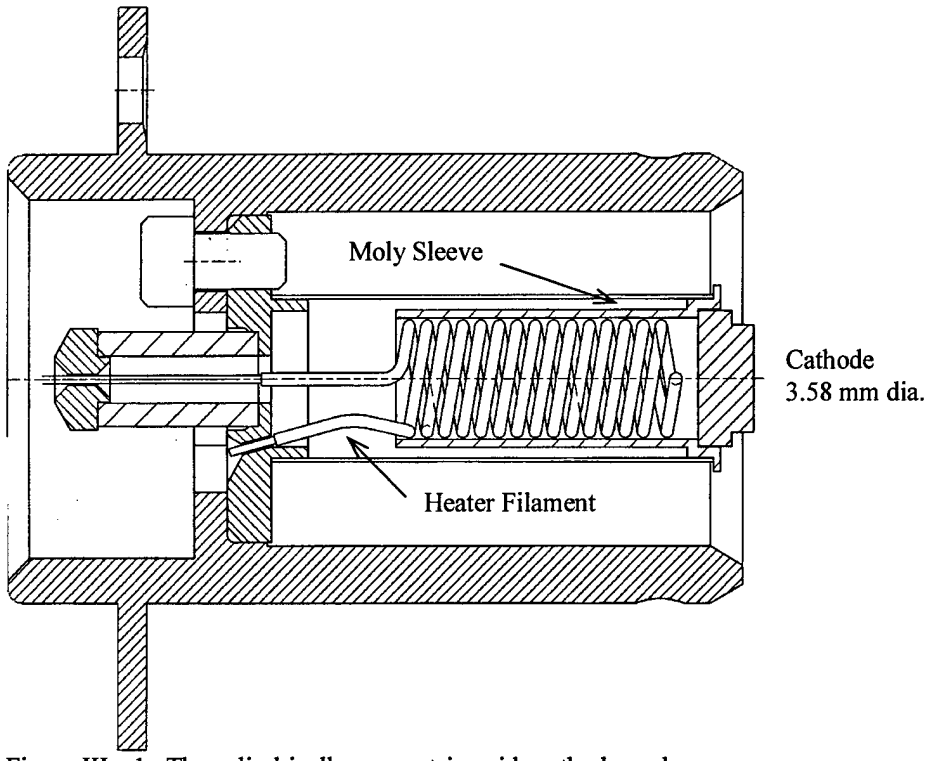

Figure III.a.1. The cylindrically symmetric oxide cathode package shown at approximately four times larger than actual size.

The emitting surface is the button on axis at the far right of the drawing, and it is heated by the coiled resistive filament (30 W maximum input power) enclosed in a molybdenum sleeve just beneath the cathode button. The remaining details of the package were designed for connecting appropriate leads, mounting and transfering the package in vacuum, and supporting the focus electrode/anode package that docks with this cathode package. The focus electrode/anode package is based upon the Varian/CPI design utilized for many years in their cathode life test vehicles.

All parts that are exposed to high temperatures (up to 1000°C) and which are located near the cathode are manufactured from high melting point molybdenum or a molybdenum/rhenium alloy in order to limit evaporation of material onto the cathode

surface or any other surrounding surfaces. Initially, some of the cathode packages were assembled using a copper/gold braze material, but it was found that the vapor pressure of this braze material at the elevated operating temperatures of these cathodes was significant enough to leave visible deposition of copper onto any surrounding surfaces. Therefore, the braze material was switched to a moly/rhenium alloy that required a higher temperature to achieve the joining but which did not evaporate as readily at the cathode operating temperature. In place of a brazed connection, a laser spot weld joint was employed to attach the nickel button to the support sleeve.

The nickel cathode buttons are not pure nickel; rather, they are slightly doped with impurities that help to activate an oxide cathode by accepting oxygen atoms from a barium oxide molecule. This oxygen transfer subsequently creates free barium which may migrate to the surface of the oxide cathode to help form the monolayer of free barium that is believed to be critical to optimum perfomance of an oxide cathode. Two different types of cathode nickel were employed in the current experiments. The alloy known as 129 nickel is doped with roughly 3.7% tungsten (by weight) as well as with small amounts of iron, magnesium, and silicon (each at less than 0.08% by weight) as determined by glow discharge mass spectroscopy analysis of two samples taken from the stock used for these experiments. The other cathode nickel employed herein, 230 nickel, contains smaller amounts of a wider variety of activating agents. Glow discharge mass spectroscopy of a 230 nickel sample showed manganese, magnesium, carbon, silicon, cobalt, and aluminum in amounts that ranged from 0.09% for manganese down to 0.02%

for aluminum. Both cathode nickel formulations have been previously used with success in the past as oxide cathode substrates.

The cathode package described above was masked before depositing the barium and/or strontium oxide layer by exposing only the nickel button surface to the plasma. After deposition, the mask was removed and the cathode package was docked into its focus electrode/anode companion piece so that the cathode could be activated and current could be drawn.

III.b. Theory of Space Charge Limited Emission

Given an infinite source of electrons, there is still a limitation to the amount of self-consistent current one may draw from a cathode to an anode for a given potential difference between the two electrodes. A derivation of the Child-Langmuir law for space charge limited flow is given here for infinite parallel plane electrodes,[1] but the results are easily adapted for other geometries such as the cathode-anode geometry of the package employed in this experiment and described earlier.

A few clarifying assumptions are first worthwhile. A steady-state solution is sought; thus, all partial derivatives with respect to time are zero. It is also assumed that electrons are emitted from the cathode with zero initial velocity and that each of their paths is along a straight line trajectory towards the anode (z-direction motion only). The potential at the cathode plane is chosen to be zero while the potential at the anode (some

set distance) away is a positive fixed value. Given these assumptions and boundary conditions, one may then seek a solution to the following three equations:

$$\nabla^2\varphi = \frac{d^2\varphi}{dz^2} = -\frac{\rho}{\varepsilon_0}, \qquad \text{(Poisson's equation)}$$

$$J_z = \rho\dot{z} = const, \qquad \text{(continuity equation)}$$

$$\frac{1}{2}m_e\dot{z}^2 = e\varphi(z). \qquad \text{(equation of motion)}$$

Substituting the expression for $\dot{z}$ from the equation of motion into the continuity equation and solving for the current density, ρ, yields

$$\rho = \frac{J_z}{\dot{z}} = J_z\left(\frac{m_e}{2e\varphi(z)}\right)^{1/2}$$

so that Poisson's equation becomes

$$\frac{d^2\varphi}{dz^2} = \frac{J}{\varepsilon_0}\sqrt{\frac{m_e}{2e}}\left(\frac{1}{\varphi}\right)^{1/2}$$

where $-J_z$ has been defined as the positive current density, J. If both sides of this equation are multiplied by $d\varphi/dz$, then one can integrate to arrive at

$$\left(\frac{d\varphi}{dz}\right)^2 = \frac{4J}{\varepsilon_0}\sqrt{\frac{m_e}{2e}}(\varphi)^{1/2} + C.$$

Here we consider only the special case where $d\varphi/dz = 0$ at $z = 0$. Thus, since $\varphi = 0$ at $z = 0$, it is determined that $C = 0$ as well. After taking the square root of the equation above, a second integration then yields

$$\frac{4}{3}\varphi^{3/4} = 2\left(\frac{J}{\varepsilon_0}\right)^{1/2}\left(\frac{m_e}{2e}\right)^{1/4} z$$

or

$$\varphi = \left(\frac{3}{2}\right)^{4/3}\left(\frac{J}{\varepsilon_0}\right)^{2/3}\left(\frac{m_e}{2e}\right)^{1/3} z^{4/3}.$$

Since $\varphi = V_0$ at $z = d$, one then arrives at the following expression for V_0

$$V_0 = \left(\frac{3}{2}\right)^{4/3}\left(\frac{J}{\varepsilon_0}\right)^{2/3}\left(\frac{m_e}{2e}\right)^{1/3} d^{4/3}$$

which may be solved for the space charge limited current density[1]

$$J = \frac{4}{9}\varepsilon_0\left(\frac{2e}{m_e}\right)^{1/2}\frac{V_0^{3/2}}{d^2}. \qquad \text{(Child-Langmuir law)}$$

Thus, the maximum current density drawn is proportional to the 3/2 power of the applied voltage and varies inversely as the square of the separation distance between the two parallel plane electrodes. For different electrode geometries, the functional dependence of the current on the voltage remains the same; only the proportionality constant changes. Thus, for a fixed electrode geometry, the relation is often written

$$I = PV^{3/2}$$

where the geometry of the structure determines the perveance, P, of the structure. When a thermionic emitter is hot enough to have sufficient free electrons available, the current drawn from it is very nearly proportional to the applied voltage raised to the 3/2 power. In the current experiment, the Varian/CPI electron gun was designed for a microperveance (μP) of two (as verified by years of personal experience of George Miram of Varian/CPI; the additional complications introduced by the gun's cylindrical geometry and hollow anode preclude a theoretical determination of the perveance here.

Nevertheless, a rough estimate may be calculated using the relation derived above for parallel plane geometry. For an emission area of 0.1 cm^2 and a cathode-anode separation distance of 0.274 cm, the calculated perveance is 2.2 μP). As is evident from the Child-Langmuir law above, this perveance may be de-rated by an increase in the cathode-anode separation distance. Since the cathode and anode packages are held together only by friction in the current experiments, thermal expansion of the parts away from each other often de-rated the microperveance to as low as one (part of this de-rating may also be due to localized non-emission sites on the cathode surface which change the assumed cathode-anode geometry). For a thermionic emitter, the Child-Langmuir law for the space charge limited emission from a set of electrodes is only valid when there are a sufficient number of free electrons available for carrying the current. Determining the number of such electrons for a given temperature is the subject of the next section.

III.c. Theory of Temperature Limited Emission

For reliable, steady operation, thermionic cathodes in linear microwave devices are operated in the fully space charge limited regime so that the current follows the 3/2 power law derived above (in contrast, non-linear tube devices such as the gyrotron operate with the cathode in the temperature limited regime). If the work function of the cathode rises or the operating temperature of the cathode is decreased sufficiently so that there are no longer enough thermally liberated electrons to allow the current to keep up with the 3/2 power law, the cathode enters the temperature limited regime.

Thermionic emission may be predicted by examining the electrons near the surface of a metal. Such electrons obey the Fermi-Dirac probability distribution function given by

$$f(E) = \frac{1}{e^{(E-E_f)/k_B T} + 1}$$

where E is the energy of an electron, E_f is the Fermi energy for the particular metal, k_B is the Boltzmann constant, and T is the absolute temperature of the metal. For typical cathode operating parameters, the exponential term dominates the denominator and the expression simplifies to

$$f(E) = e^{-(E-E_f)/k_B T}.$$

Only electrons with energy greater than the sum of the Fermi energy (required to enter the conduction band) plus the energy required to liberate themselves from the cathode surface will have a chance at participating in current flow from the anode to the cathode.

As before, parallel planar geometry is assumed for the electrodes, so the quantity of interest is the z-component of the current density, J_z, which is given by the product of the electron charge, the electron velocity in the z direction, and the number per cubic meter of electrons with sufficient momentum in the z direction to overcome the potential barrier of the surface work function. Within a differential element of three-dimensional momentum space, the current in the z direction is then

$$d^3 J_z = e v_z \frac{2}{h^3} f(E) dp_x dp_y dp_z$$

where h is Planck's constant and the factor of $2/h^3$ is the required normalization factor. Since the distribution function, $f(E)$, is as given above and the energy of each electron is just $E = (p_x^2 + p_y^2 + p_z^2)/2m_e$, the differential current may then be integrated over all of momentum space with the restriction that only those electrons with $p_z \geq p_{z\min} = \sqrt{2m_e(E_f + e\varphi)}$ (φ is the work function) have sufficient momentum in the z direction to participate in current flow. After writing all energies and velocities in terms of momentum, the current in the z direction then becomes

$$J_z = \frac{2e}{m_e h^3} \int_{-\infty}^{+\infty} \exp \frac{-p_x^2}{2m_e k_B T} dp_x \int_{-\infty}^{+\infty} \exp \frac{-p_y^2}{2m_e k_B T} dp_y \int_{p_{z\min}}^{+\infty} \exp \frac{-p_z^2}{2m_e k_B T} p_z dp_z$$

which, upon integration (and dropping the subscript on J_z), yields

$$J = \frac{4\pi m_e e k_B^2}{h^3} T^2 e^{-e\varphi/k_B T} = 120 T^2 e^{-11.6x10^3 \varphi/T} \text{ (Richardson-Dushman)}$$

where J is measured in amperes per square centimeter for T given in degrees Kelvin. With either a sufficiently high operating temperature or a sufficiently low work function, the predicted temperature limited current density begins to exceed the space charge limited current density for a given operating voltage, and the cathode then operates fully space charge limited with the current following the 3/2 power law.

The Richardson-Dushman equation is the foundation for evaluation of thermionic emitters with a work function given by φ operating at a temperature T. For a real cathode, φ is actually a function of both position (due to surface variations) and temperature (due to changing cathode chemistry and evaporation rates). Thus, in practice, both the current density and the temperature of the cathode are varied and

measured, and effective work function distributions associated with these parameters may be calculated. These work function distributions may then be used to make predictions about both the maximum achieveable current density for an acceptable operating temperature as well as the uniformity and overall quality of the cathode. Key to these predictions are both the temperature and current measurements, the subjects of the following two sections.

III.d. Temperature Measurement of Cathodes

Due to the small cathode package size and the high voltages involved, mounting a thermocouple for measuring the cathode temperature is impractical. Instead, common practice is to measure the cathode temperature using an optical pyrometer. In the current work, a Leeds-Northrup hot wire pyrometer is employed to measure the cathode temperature by matching the visible color of a wire in the viewfinder to the visible color of the cathode surface. The hot cathode is viewed through a standard glass viewport on the vacuum chamber. Care must be taken to ensure that the viewport does not become coated with any activation products or any other material which may evaporate off of the cathode package and form a thin film on the viewport glass (such a film reduces the transmission of the cathode glow to the pyrometer and alters the apparent temperature reading). As such, the viewport through which the temperature is measured has venetian blind shutters that are only opened during a temperature reading.

The pyrometer is calibrated for the emissivity of a hot tungsten wire, so the brightness temperatures quoted throughout this work may deviate from the true temperature by as much as a couple of percent due to the different emissivity of the cathode surface. The subjectiveness of the color matching also introduces up to several percentage points of error, so the standard method for determining cathode temperature is to obtain several data points of cathode temperature versus heater filament current and to then fit the data linearly. Such a fit for a typical cathode package is shown below in Fig. III.d.1.

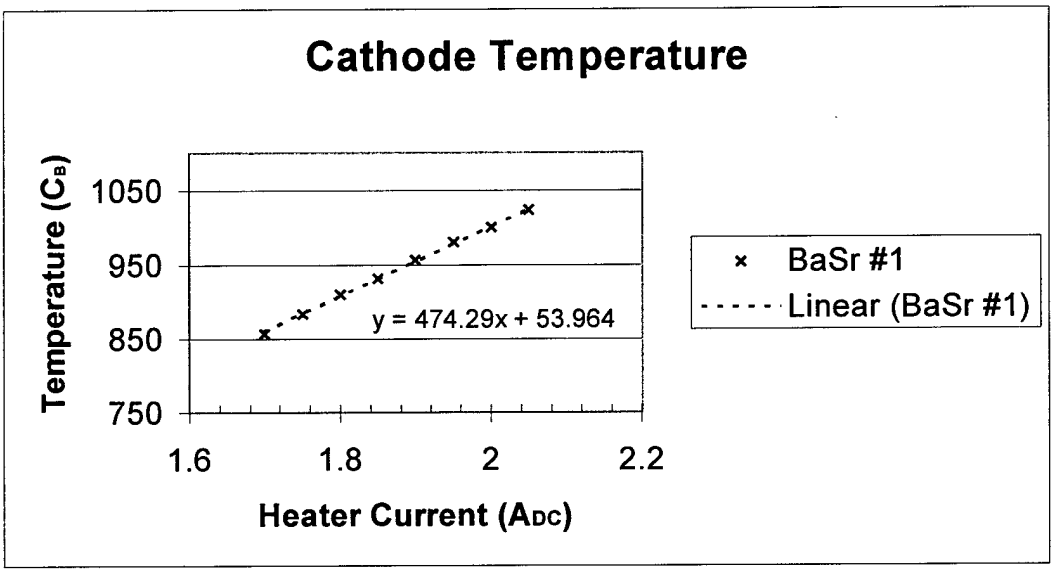

Figure III.d.1. Cathode brightness temperature as a function of current supplied to the heater filament.

Such data need only be taken once for a given cathode package after which the cathode operating temperature can be calculated given the filament current. In the current work, a heater filament was often reused a few times for different cathode packages, and small drifts were seen in the temperature versus current lines. Thus, for each cathode package, the pyrometer was used to determine the best linear relationship between the temperature

and current. The pyrometer measures brightness temperature down to 750°C, but it was found that measurements at such a low temperature were much more difficult to repeat with accuracy due to the dimness of the cathode image in the pyrometer. As such, only data above 850°C are used to determine the temperature/current relationship. The upper limit on the temperature measurements is set by the rate of evaporation of the oxide coating. Above 1000°C, the coating evaporates rapidly (typical operating temperature for an oxide cathode is between 750 and 900°C), so the present cathodes were only occasionally heated to above 1000°C.

III.e. Cathode Current Measurements

In addition to the cathode temperature, one must also know the emission current in order to determine the cathode work function. To draw emission from the cathode, two power supplies are needed: one to supply current to the heater filament and one to supply the potential difference from the anode to the cathode. Because of the close proximity of the heater filament to the cathode, the filament is held at nearly the same potential as the cathode to prevent arcing. In fact, one of the legs of the heater filament is connected to the cathode so that the two heater leads that are attached to high voltage feedthroughs on the vacuum chamber serve as both the series load for the heater supply as well as the necessary connection to the cathode for applying a large negative voltage (with respect to the grounded anode).

Initially, each cathode is tested using an AC heater supply and a DC high voltage supply. The AC heater current passes through an isolation transformer so that the DC high voltage is not seen by the 110 VAC input signal. The heater current, cathode current, and cathode voltage are all monitored using standard hand-held multimeters. Upon completion of successful DC testing, the cathode is pulse-tested using the custom designed Miram Curve Generator power supply. The MCG-200 (built by Electromatic, Inc. according to the oxide cathode program specifications) is a high voltage pulsed power supply with an integrated floating DC heater filament supply. The heater supply is capable of delivering up to 10 A of current at up to 15 V (the present filaments drew just over 2 A for cathode temperatures near 1000°C). The pulsed power supply is adjustable from 5 kV to 30 kV and can deliver up to 10 A of pulsed current. Pulse widths are variable from 0.4 to 10 μsec with available single shot to 1 kHz repetition rates.

Connection is made to the cathode package inside the chamber via the copper wire leads that run from the package to the high voltage feedthroughs mounted on a single 6" Conflat flange on the chamber. Two 40 kV feedthroughs were placed on a 6" flange. Each feedthrough can stand off 40 kV from the feedthrough to the flange, but because of the close proximity of the feedthroughs to each other, they may not withstand a 40 kV potential difference between themselves. The stand off available between the two is not an issue since the only voltage drop across them is the voltage dropped across the heater filament (always less than 10 V in the current experiments). From the air side of the feedthroughs, connection is made to the high voltage DC supply and the AC heater supply via standard 600 V insulated wire (the maximum DC high voltage applied to the

cathode is 450 V). When the switch is made to pulsed operation, the air side leads are two heavy gauge coaxial cables from which the outer conductor has been stripped leaving just the center conductor surrounded by roughly 3 mm thickness of insulating material. These leads are run through a grounded metal conduit to the Miram Curve Generator (the total length of each lead is roughly 7 meters). Pulsed voltage is measure by placing a high voltage oscilloscope probe (same as discussed in Sect. II.d.) at the cathode feedthrough, and pulsed current is measured using a pulsed current transformer through which both the leads are run so that the current flowing from the anode to the cathode is measured while the current flowing through the heater filament cancels itself out (again, this current transformer is described in Sect. II.d.).

To verify proper operation of a cathode, the cathode is first heated to a nominal operating temperature of 900°C, at which point the I-V characteristic of the cathode is investigated. For space charge limited operation, the current should follow the 3/2 power law derived earlier. As the applied voltage increases, eventually there are not enough thermally liberated electrons to maintain the 3/2 power law, and the current begins to level off with increasing voltage. A set of I-V curves for a good cathode are shown in Fig. III.e.1.

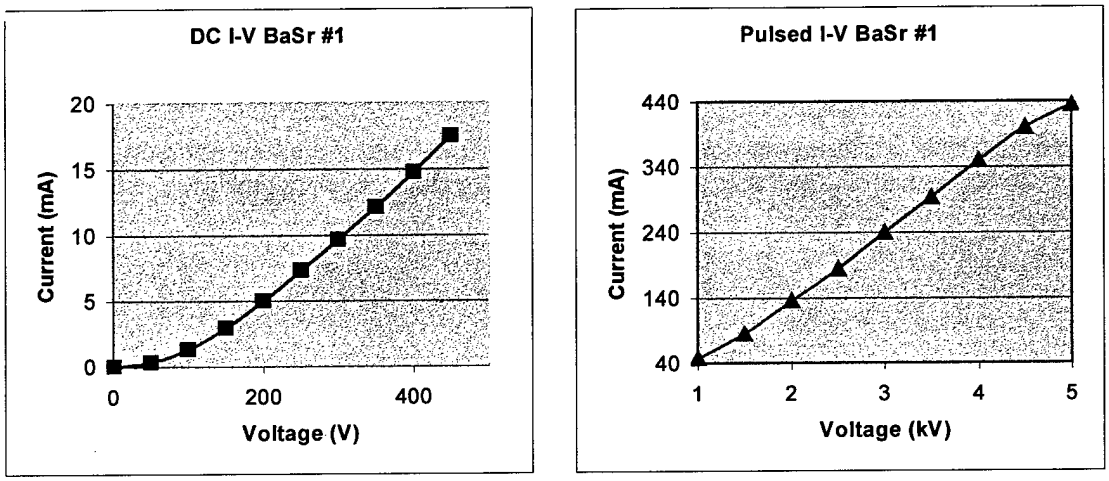

Figure III.e.1. I-V characteristic for cathode BaSr #1. Cathode temperature for both curves is approximately 910°C.

The DC I-V curve shows that the cathode is operating fully space charge limited since the current closely follows the 3/2 power law above 100 V (the mean perveance calculated from this data is 1.80±0.03 μP which is 10% below the designed perveance most likely as the result of slight geometry changes that take place during thermal expansion). When applied voltage is increased in the pulsed I-V curve, the current begins to lag behind the 3/2 power law as the emission becomes temperature limited. The calculated perveance decreases to as low as 1.2 μP when pulsed at 5 kV at this temperature. Adherence to the 3/2 power law of the space charge limited regime may be recovered by simply increasing the cathode temperature.

After verifying proper cathode performance, data are collected in order to generate what is known as a Miram curve (named after Varian/CPI cathode specialist George Miram). Miram curves provide a "practical" work function distribution function (not a true work function since the method of generating the curve follows an experimental rather than theoretical prescription). To generate a Miram curve, one first

fixes the applied voltage and verifies that the cathode is operating fully space charge limited. Then, the cathode temperature is gradually decreased while monitoring the cathode current. As the cathode cools, it eventually begins to operate temperature limited and the current decreases with decreasing temperature. Each point on this current versus temperature roll-off is then used to calculate a work function using the Richardson-Dushman formula derived in Sect. III.c. (solved for the work funciton, φ):

$$\varphi = -\frac{T}{11.6x10^3}\ln\left(\frac{J}{120T^2}\right)$$

where φ is in eV for T in degrees Kelvin and J in A/cm^2. Under normal experimental conditions, the calculated practical work function decreases slightly with decreasing temperature, so the various practical work function values may be plotted according to Miram's prescription to yield a practical work function distribution (PWFD).[2] One such set of roll-off and PWFD data is shown in Fig. III.e.2.

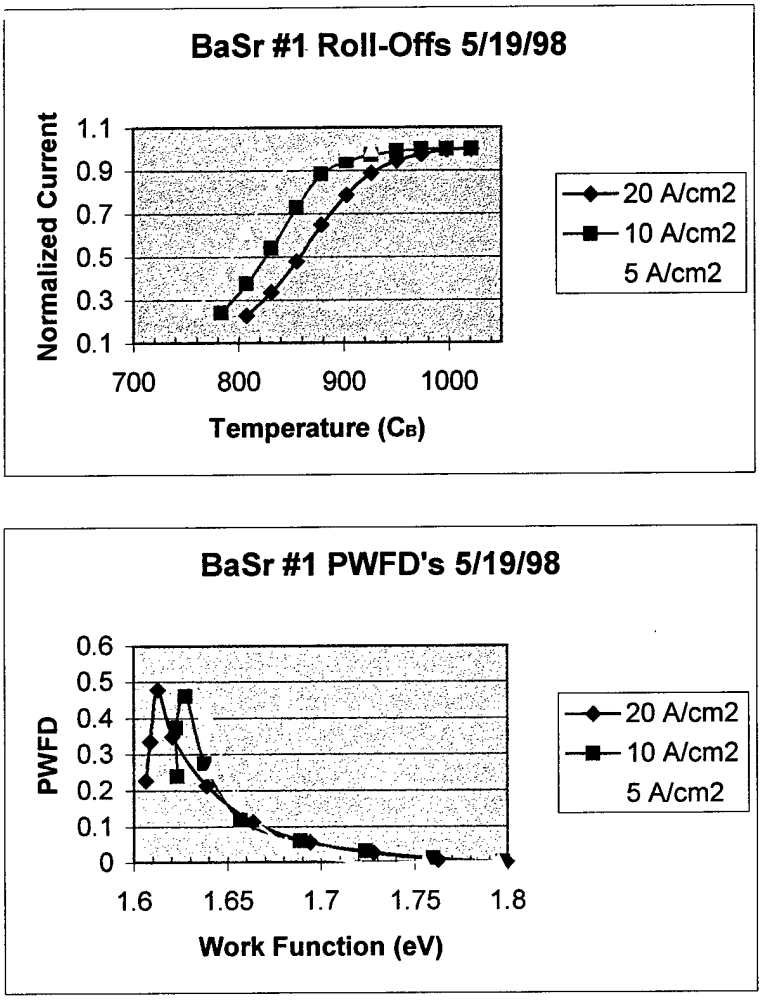

Figure III.e.2. Roll-off (upper) and practical work function distribution (lower) data for a combination barium and strontium oxide cathode manufactured via vacuum arc deposition.

As seen in the figure above, achieving higher current densities requires operating the cathode a higher temperatures. The corresponding practical work functions for the roll-offs then lie between 1.61 and 1.65 eV at their peaks. The peak location as well as the shape of the distribution provide valuable information on the quality of the particular cathode. Lower work functions correspond to being able to draw larger currents at low

operating temperatures (for long life), and narrow distributions imply uniformity of the cathode surface and the emission sites. PWFD data are collected on each cathode that performs well enough to get a valid roll-off. Detailed analysis of these results as well as the process used to attain them are the subject of the next chapter, Results & Discussion.

IV. RESULTS & DISCUSSION

In July of 1996, the UC Davis/Stanford Linear Accelerator Center (SLAC) team began working directly with Dr. Ian Brown of Lawrence Berkeley National Laboratory (LBNL) to evaluate the feasibility of using vacuum arc plasma deposition to create oxide cathodes. Several test depositions were done in order to develop expertise working with the highly reactive barium metal as a plasma source. Eventually, attempts to deposit barium on a clean silicon substrate met with success.

Following the success of the initial barium depositions, the UCD/SLAC/LBNL collaboration designed an experimental set-up whereby both the deposition and cathode activation could take place in the same vacuum chamber. A standard 1" diameter klystron cathode package was employed as the substrate for deposition of approximately 0.7 microns of barium oxide. Immediately following the deposition, the cathode was placed a distance 0.5" from a planar copper anode/collector. The cathode was subsequently heated to temperatures between 770°C and 870°C where the pulsed current emission was monitored at cathode/anode voltage differences up to 2 kV. Results from this initial effort are shown in Fig. IV.1. Despite the thinness and nonuniformity of the coating, a maximum current of 1 A was achieved--well beyond expectations. The nonuniformity of the coating was due to the large size of the substrate surface compared to the plasma source (1" diameter substrate vs. a 1/4" diameter barium rod). Following the success of this proof-of-principle experiment, facilities for manufacturing and testing

plasma deposited oxide cathodes were assembled at UC Davis (and subsequently moved to SLAC) in order to further pursue this novel method for making oxide cathodes.

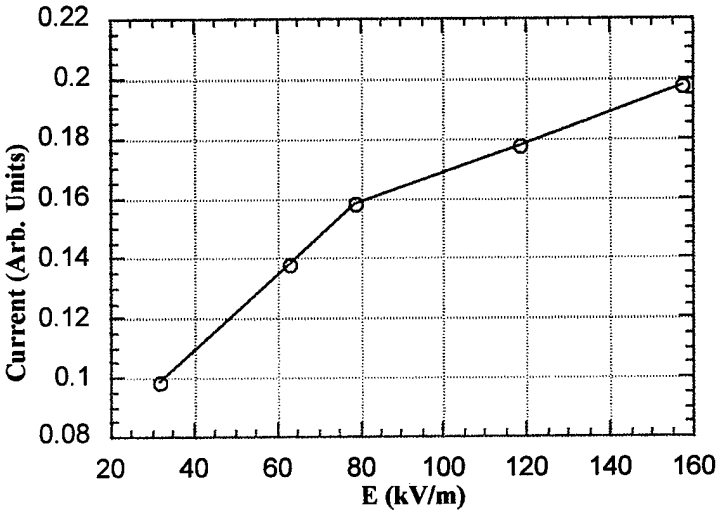

Figure IV.1. Temperature limited current drawn from the first vacuum arc deposited oxide cathode at LBNL. Cathode temperature was 815°C.

In this chapter are details on the follow up experiments performed using the vacuum arc deposition and cathode testing equipment described in the previous two chapters. First, the process steps that led to noteworthy oxide cathodes are detailed, followed by the presentation and analysis of data from these cathodes. Finally, descriptions of failed attempts at oxide cathodes are given together with proposed problem sources and their corresponding solutions.

IV.a. Making an Oxide Cathode

Successful manufacturing of an oxide cathode requires a high level of cleanliness and careful preparation. Before loading a cathode package or anode package into the vacuum chamber, the parts are vacuum fired to encourage outgassing (especially of the hydrogen adsorbed on the surfaces during a hydrogen brazing process).

If a new barium/strontium-filled nickel tubing plasma source is needed, it is first unpacked from the mineral oil in which it is shipped (source rods are purchased from ACI Alloys in San Jose). Then, the rod must be turned down on a lathe to 0.249" in diameter so that it fits snugly into the ceramic insulator that holds it. The rod may then be cleaned with mineral spirits (paint thinner), but not with acetone or ethanol (barium and strontium both react with most solvents).

The deposition chamber is then let up to atmospheric pressure by backfilling with warm dry nitrogen (backfilling with laboratory air would introduce additional water vapor that would unneccessarily increase the time required to pump down the chamber). The lid of the chamber is removed so that complete access to the inside of the chamber is available. The fresh cathode package is then mounted on its stand, and a mask is mounted on the package that exposes only the nickel button surface to the plasma. Then, the leads for the heater and cathode are attached to the vacuum side of the high voltage feedthrough described in Sect. III.e. The shutter covering the rate thickness monitor should be open so that the crystal will be exposed to the plasma during the deposition. The previous plasma gun cathode and trigger cap are removed from the chamber and reconditioned for the next deposition. Reconditioning consists of removing deposited films from the trigger cap (using a combination of a scraping knife and a dry bead blast

procedure), replacing the ceramic insulator that holds the source rod with a cleaned insulator, and belt sanding the source rod to expose fresh barium/strontium before reassembling the plasma gun inside the vacuum chamber. During this preparation, care is taken to avoid ingesting metallic dust, and skin contact with the metallic powder is kept to a minimum. The substrate is subsequently placed in position roughly 6.0 cm from the plasma gun anode snout. A final check is made on all electrical leads inside the chamber to ensure vacuum gaps large enough to prevent any possible arcing.

Finally, the chamber lid is placed back on and the roughing pump is opened to the chamber. As the pumping is begun, warm dry nitrogen is again bled into the chamber to help sweep adsorbed water molecules off of internal surfaces. The nitrogen is shut off when the chamber pressure reaches roughly 130 Torr, and the chamber then rapidly pumps down into the millitorr range. The turbopump is activated when the chamber pressure reaches 100 mTorr. After the chamber pressure is in the 10^{-6} Torr scale (roughly half an hour after starting turbopump), the cathode package is given a bake out by bringing the heater filament current up to 1 A (roughly 500°C). To ensure a clean background for the deposition process, the chamber is allowed to pump to at or below the mid 10^{-7} Torr scale over a period of 15 to 18 hours before the deposition is performed (since the first cathode deposition at LBNL (see the beginning of this chapter) was performed in a mid 10^{-6} Torr background pressure and met with some success, an order of magnitude improvement in the background pressure should improve the overall cleanliness and repeatibility of the process).

Before beginning deposition, the water vapor partial pressure should be in the low 10^{-7} scale or below (as measured by the residual gas analyzer); excess water vapor might allow the film to deposit as a hydroxide rather than the desired oxide film. The cathode package heater filament current is reduced to 0.5 A (roughly 275°C). The cathode is kept warm during deposition and throughout subsequent transfer to the anode and testing in order to discourage absorption of water vapor by the oxide coating. A bottle of 99% Argon/1% Oxygen is attached to the chamber and a small amount is flowed through the chamber (enough to bring the chamber pressure into the high 10^{-7} scale) to ensure that there will be sufficient oxygen available to oxidize the free barium and strontium that will be deposited; pure oxygen could just as easily be used, but the mixture employed has the advantage of adding inert, easily-ionized argon to encourage successful triggering of the plasma. A sample RGA scan before deposition is shown in Fig. IV.a.1. The electronics are allowed to warm up while the Ar/O_2 flow equilibrates in the chamber. The substrate bias pulser is set for 2.25 kV output, the main arc current supply is set to 200 V, and the trigger pulser is set to output up to a 7 kV pulse (as detailed in Sect. II.c.).

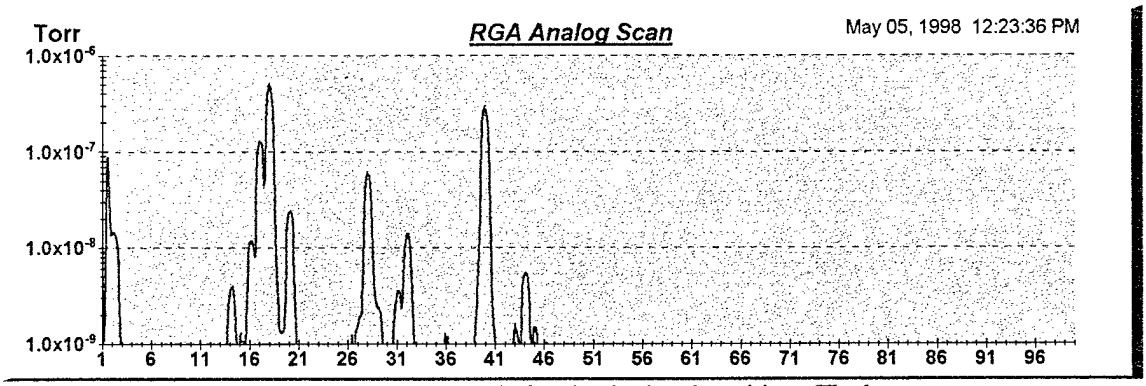

Figure IV.a.1. Residual gas analysis spectrum before beginning deposition. The large water vapor presence (16, 17, 18 peaks) is accompanied by argon (40 and 20), nitrogen (28 and 14), hydrogen (2), oxygen (32 and 31), and carbon dioxide (44).

The plasma is subsequently triggered by placing the controlling pulse sequencer in internal trigger mode (set for 1 Hz repetition rate). After the first two hundred pulses, the substrate bias pulser is lowered to output 400 V. During deposition, the optical emission spectrometer may be employed to monitor the characteristic lines emitted by the plasma. Spectra may then be compared to previous spectra in order to ensure that the same lines (and only those lines) are present. Such a comparison provides only a gross indication of the presence or lack of contaminants since any given contaminant may or may not have strong emission lines in the observed wavelength range. Several authors have previously shown optical emission spectroscopy to be a suitable technique for characterizing vacuum arc deposition.[123] In the current work, it was found that the relative intensities of the detected lines varied from shot to shot, but the lines that constituted each spectra did not change. This variation is evident in the spectra from two separate deposition runs shown in Fig. IV.a.2. This intensity variation can be explained by the changing relative abundances of the excited species in the plasma. No variation of the elemental composition of the plasma was ever detected since each spectra's constituent lines were identical.

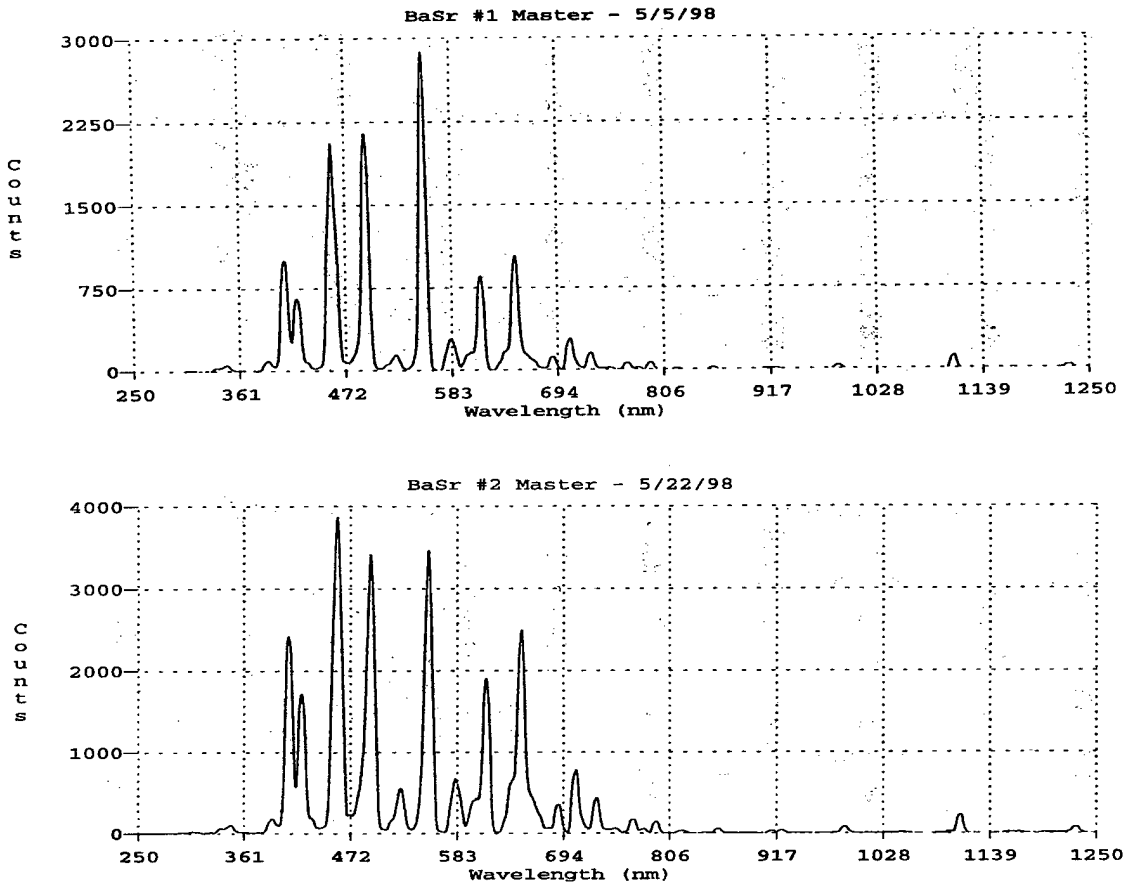

Figure IV.a.2. Optical emission spectra from two separate deposition runs. Line intensities are seen to vary, but line positions remain consistent. The 7 strongest emission lines are identified as follows: Sr+ at 407.7 nm, Sr at 421.6 nm, Ba+ at 455.4 nm, Ba+ at 493.4 nm, Ba at 553.5 nm, Ba+ at 614.1 nm, and Ba at 649.7 nm.

The process may also be monitored via the residual gas analyzer (RGA). Upon initiating the plasma, most gas partial pressures rise due to the outgassing encouraged by the intense heating of the plasma gun. Sample RGA scans from the beginning and middle of the deposition process are shown in Fig. IV.a.3. After several minutes of deposition, the background gas pressures come down, although hydrogen continues to be released. The main feature to note is the presence of methane (13, 14, 15, and 16 peaks)

that is created during deposition. In addition, various hydrocarbons are most likely formed based on the groupings of the residual gases. Oxygen rapidly disappears from view, and water vapor is significantly reduced due to the barium and strontium gettering.

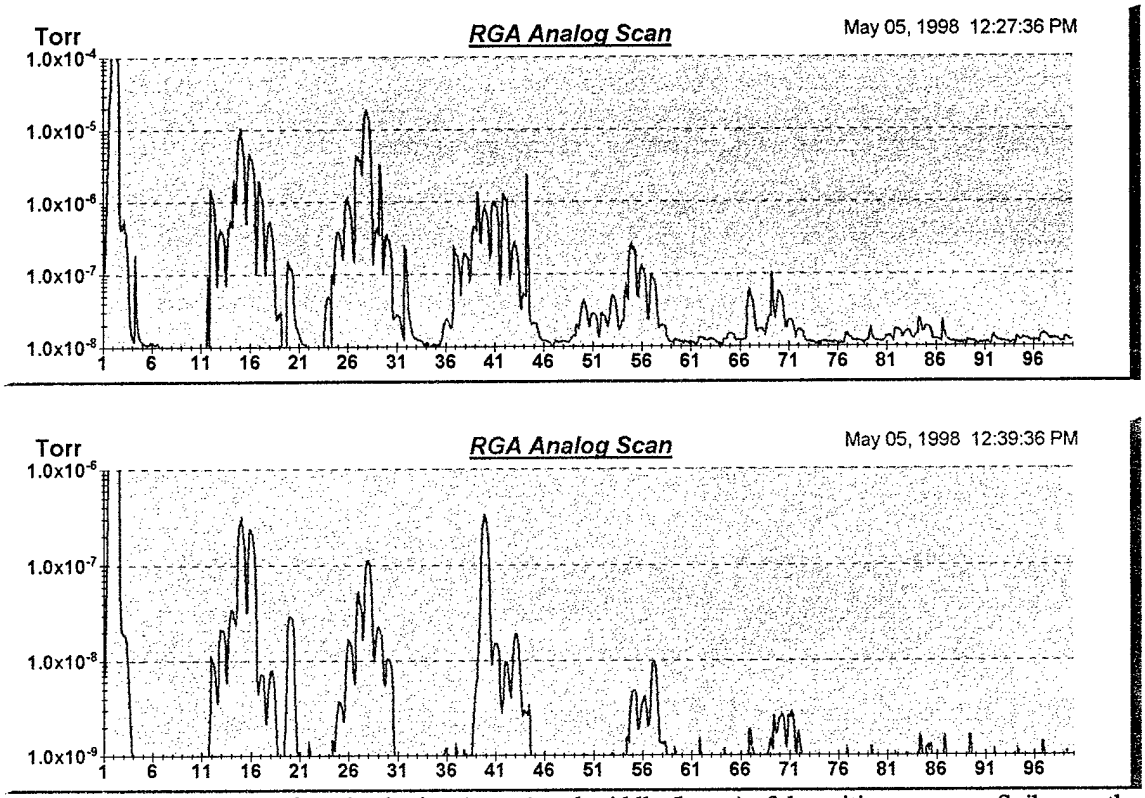

Figure IV.a.3. RGA scans from beginning (upper) and middle (lower) of deposition process. Spikes on the data are not real but rather noise induced by the pulsed plasma.

Yet another available tool for analyzing the deposition plasma is the electrostatic plasma probe (ESP) described in Sect. II.d. In order to minimize the deposition perturbations that introducing the probe into the plasma may cause, the ESP data is collected during plasma shots that were not used to make a cathode. Sample ESP data and the analysis results are shown in Fig. IV.a.4. Data for the electron temperature and number density fall within the ranges reported elsewhere[4] for vacuum arc deposition of titanium nitride.

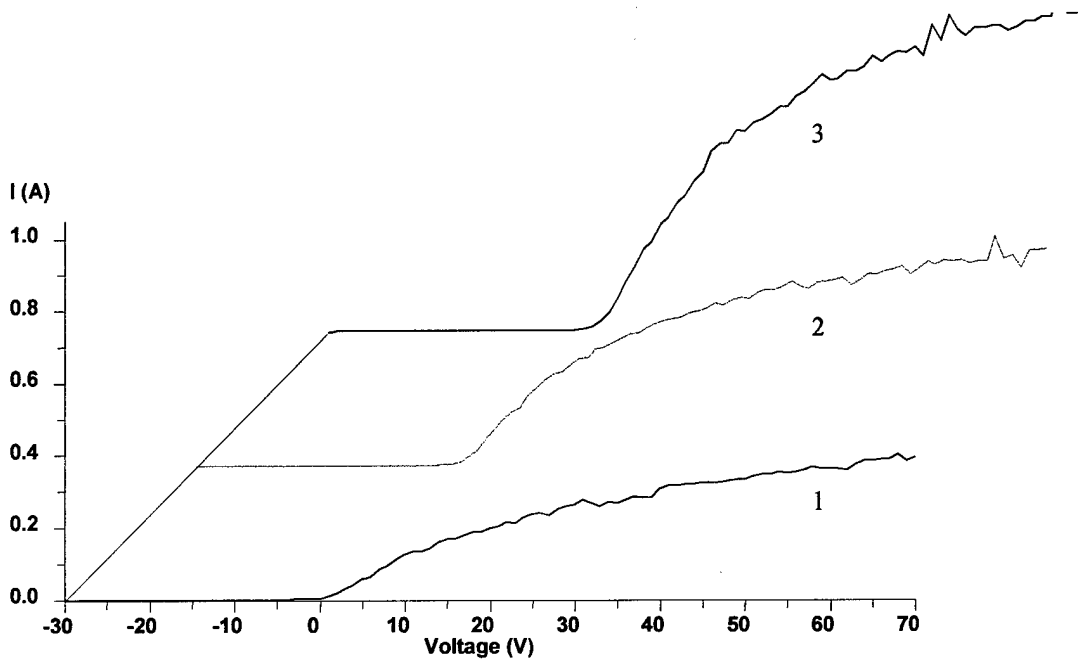

Scan	Position (cm)	Plasma Potential (V)	Electron Temperature (eV)	Ne (x 10^{12} cm^{-3})	Ni (x 10^{12} cm^{-3})	Debye Length (μm)
1	19	5.41	1.25	1.66	0.72	6.46
2	20	5.36	1.16	2.88	1.13	4.73
3	21	6.24	1.30	4.77	1.87	3.89

Figure IV.a.4. ESP I-V scans and analysis results for three different probe tip positions approaching the center of the plasma. Data is taken during a pulsed barium plasma.

As the probe tip approaches the plasma center, it begins to draw more than 1 A of electron current at saturation. Since this probe is only capable of handling up to 1 A of current, the scans are halted before reaching the plasma center (which would correspond to a position of 25 cm). Thus, this probe data examines only the outer edges of the deposition plasma. A fitting routine is used on each I-V curve to arrive at calculated values for the parameters shown in the table. From the ratio of the electron density to the ion density, it is seen that the average ionization level of the ions in the plasma is between +2 and +3. To probe the plasma center, the probe tip would have to first be much reduced in area so that it collects less than 1 A of current at maximum positive bias.

The plasma is also monitored visually by the bright flashes visible through any of the chamber viewports. The trigger current and plasma arc current are displayed on the local oscilloscope, and the rate thickness monitor tracks both the number of angstroms per second deposited as well as the total accumulated thickness. A pulse counter keeps track of the number plasma shots fired, and the process is stopped at shot #1000 (which corresponds to between 1 and 5 microns of coating; each shot deposits roughly 1 to 5 nm of coating). Within a few minutes, the Ar/O_2 flow is stopped, and the chamber is allowed to pump down (usually to the low 10^{-7} or high 10^{-8} Torr scale due to the gettering performed by the free barium and strontium). As is seen in Fig. IV.a.5, the post-deposition RGA spectrum shows considerably fewer constituent gases, but with a large methane presence that was non-existent before depostion. The heater filament current for the cathode package is maintained at 0.5 A while the preparations are made for opening the chamber and docking the cathode into an anode structure for testing.

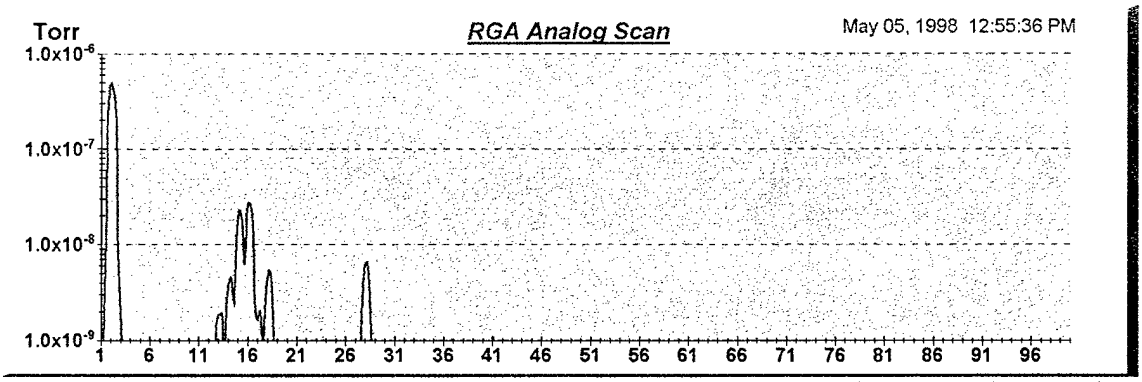

Figure IV.a.5. RGA spectrum following deposition (the argon/oxygen flow is off). Large hydrogen and methane (16, 15, 14, 13) presences dominate, while water vapor (18) and nitrogen (28) make up the rest of the background gas.

IV.b. Testing an Oxide Cathode

After successful deposition of 1,000 plasma shots onto the cathode substrate, the mask must be removed and the cathode docked into an anode structure before testing of the cathode can begin. In order to accomplish these tasks, the vacuum chamber must be brought up to atmospheric pressure and the lid removed to provide full access to the cathode package. Unfortunately, oxide cathodes are highly susceptible to poisoning by exposure to the ambient water vapor. The oxides readily convert to hydroxides ($Ba(OH)_2$) and their hydrates ($Ba(OH)_2 \bullet nH_2O$) which refuse to reconvert back to oxides upon subsequent heating. Studies have been performed where oxide cathodes were exposed to air while they were kept hot, and it has been found that by keeping the oxide coating temperature elevated to 150 to 200°C the formation of the hydrates may be prevented thereby permitting near full recovery of the emission.[5] Thus, while backfilling the chamber with warm dry nitrogen, the cathode heater filament current is maintained at 0.5 A (roughly 275°C at the cathode surface); if the filament current is too high, the hot filament oxidizes when exposed to air, and the coils shed their insulating coating thereby shorting out the heater filament.

After the chamber is completely backfilled with warm nitrogen, the lid is removed and the purge is left running. The mask is removed from the cathode package, the coating is visually inspected, and then the cathode package is docked into the anode package and aligned in the chamber such that the cathode surface is visible from a 6" viewport. The stainless steel panel that is employed to protect the electrical feedthroughs from the deposition plasma is then moved in front of the plasma gun so that the plasma

gun has no line of sight to the docked cathode-anode package (this is important to the gas gettering that is performed later by firing the plasma gun). The nitrogen purge is turned off just before closing the chamber lid (so that positive pressure does not distort the o-ring seal), and the roughing pump is opened up to the chamber. The total time that the lid is removed should be kept as short as possible (under five minutes) in order to limit the amount of air exposure received by the cathode. As the pressure comes down, the nitrogen purge is initiated again and allowed to run until the chamber pressure is roughly 130 Torr. Then, the purge gas is shut off, and the turbo pump is started after the chamber pressure reaches 100 mTorr. After the pressure has entered the 10^{-6} Torr scale, the cathode heater filament current is raised to 1 A (roughly 500°C) to help begin baking out the cathode and anode packages while the system pumps down. Activating and testing the cathode is not undertaken until the chamber pressure is in the low 10^{-7} Torr scale (typically a few days of pumping).

The residual gas components play key roles in the cathode quality not just during deposition but during activation and test as well. Having a low background pressure is critical for low work function cathodes to perform since they may operate at lower temperatures and thereby be more susceptible to poisoning. Before beginning activation, water vapor partial pressure should be in the mid 10^{-8} Torr scale or below. In the current work, the heater filament current is brought up in steps of 0.1 A from 1 A up to roughly 2 A (almost 1000°C). At each step, the residual gas in the chamber is monitored since the heating will cause any carbonates to convert into oxides (as is the case with traditionally manufactured oxide cathodes). An RGA strip chart showing the partial pressures of

various gases during this heating process is shown in Fig. IV.b.1 together with RGA spectra from before and after the heating.

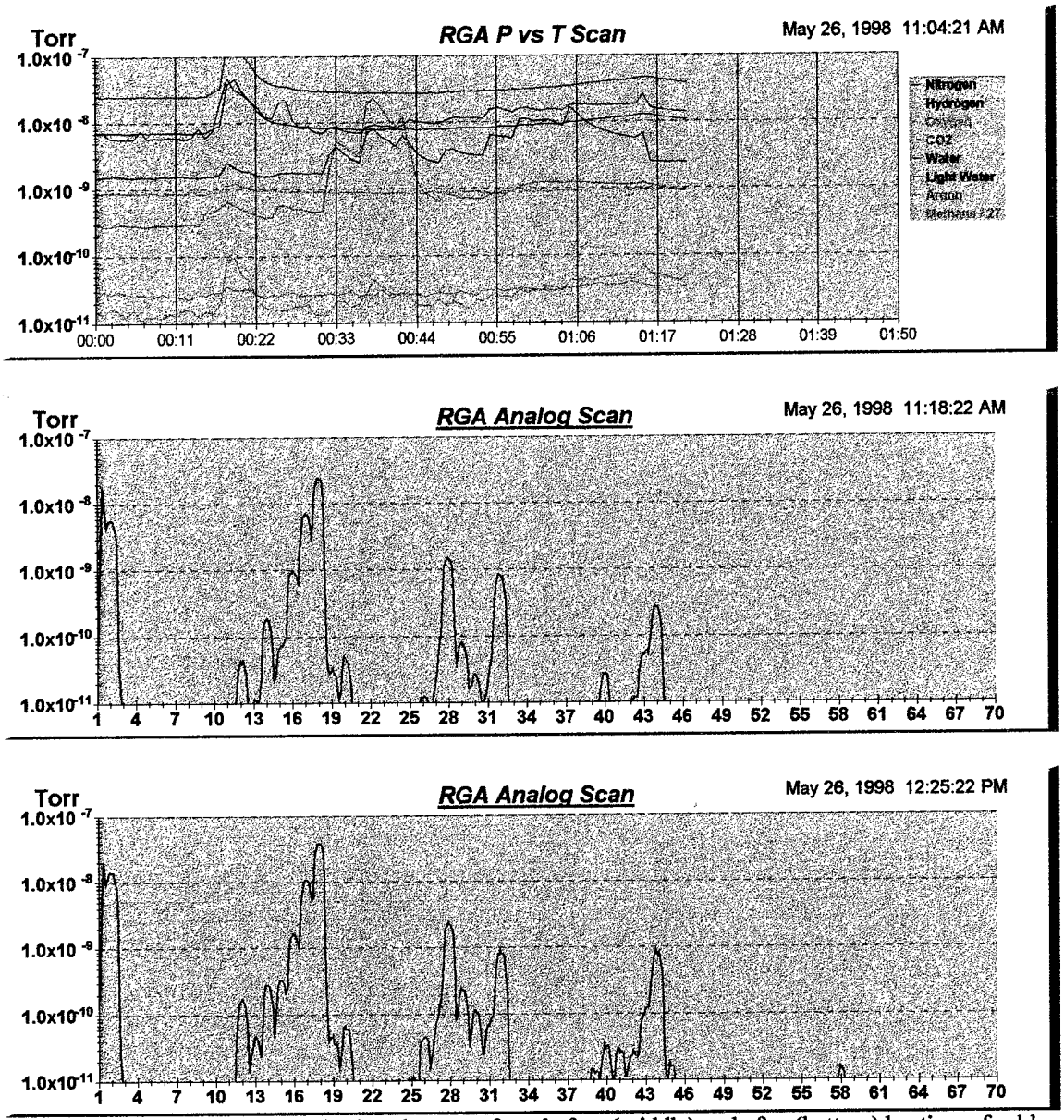

Figure IV.b.1. RGA strip chart (top) and spectra from before (middle) and after (bottom) heating a freshly deposited oxide cathode.

The main features of interest in the strip chart data are the rises in the partial pressures of carbon dioxide and carbon monoxide (which shares the nitrogen 28 peak). The initial

rise in pressure of most of the gases is due to outgassing of both the cathode and anode packages. About 30 minutes into the heating, carbonate coversion begins (cathode temperature is roughly 700°C). Eventually, carbon dioxide evolution trails off with increased heating, but carbon monoxide evolution continues to be acutely affected by changes in cathode temperature. At the end of the heating cycle, the cathode is flashed by raising the heater filament current to 2.2 A (just over 1000°C) for 30 seconds at a time. Such flashing is often employed in traditional oxide cathodes to insure complete carbonate conversion across the entire face of the cathode. As a final step, the heater filament is reduced to 1.8 A (~890°C) before beginning to draw DC emission (at this temperature, a cathode with a work function as high as 1.8 eV will still be space charge limited rather than temperature limited for emission densities up to 2.5 A/cm^2).

It was found that excessive residual water vapor caused the oxide cathode work function to increase significantly, so before drawing emission every attempt is made to reduce the background water vapor partial pressure. One such way of removing water vapor is by gettering it using the barium/strontium plasma gun. By firing 100 to 200 plasma shots, the water vapor partial pressure may be brought from the low 10^{-8} Torr scale to the low 10^{-10} Torr scale. This decrease in water vapor partial pressure is only temporary, however, since the water vapor is still inside the chamber but trapped in another form. The water vapor pressure eventually climbs back up to the low 10^{-8} Torr scale given several hours (water vapor pressure climbs much more quickly when cathode current is being drawn since beam interception liberates adsorbed water off of surfaces).

Cathode performance was best when water vapor partial pressure was kept below 2×10^{-9} Torr during testing.

To activate the cathode, a negative DC voltage is gradually applied to the cathode (the anode is grounded) in order to verify the emission properties of the cathode. The DC power supply employed in this experiment is adjustable from 0 to 500 V output, so the cathode current is measured at various applied voltages from 50 to 450 V in order to generate an I-V curve. This I-V curve (which should follow the 3/2 power law for space charge limited operation) is then used to calculate a perveance for the gun. This perveance should match the designed 2.0 μP, but, in practice, this perveance was difficult to achieve. Thermal expansion caused the cathode and anode to drift apart and reduce the perveance of the structure, and attempts to hold the cathode and anode together led to heat sinking of the cathode that prevented uniform heating. All measured perveance values were in the range of 1 to 2 μP. After taking I-V data, the cathode emission density is set to 50 to 100 mA/cm^2 for several minutes in order to help outgas all surfaces that are subjected to electron beam interception. Upon successful completion of DC activation and testing, the cathode is then configured for pulsed emission testing.

Using the Miram Curve Generator described in Sect. III.e., the cathode is tested in pulsed operation in order to generate practical work function distributions. Pulse lengths used in the current work are between 2 and 10 μsec with duties between 0.0001 and 0.001. Within this range, no correlation between pulse length/duty and cathode performance was seen. The cathode is heated to roughly 900°C and its I-V curve is established so that it may be determined at what current density the cathode begins to

operate temperature limited rather than space charge limited; this transition is evidenced by the inability of the cathode current to keep up with the 3/2 power law when the voltage is increased. The highest space charge limited emission density achieved at this temperature is then the upper limit for the roll-off. The cathode voltage is then fixed and the filament current is increased slightly to insure that the emission is truly space charge limited. Given space charge limited emission, the cathode temperature is then gradually decreased while the cathode current is measured at each temperature step (with the voltage held constant). This current vs. temperature roll-off is then employed to calculate a practical work function distribution as described in Sect. III.e. Roll-offs for other emission densities may be performed as well by adjusting the applied cathode voltage. Again, for the lowest work function results, the water vapor partial pressure had to be kept below 2×10^{-9} Torr during testing. This upper limit was accomplished by repeating the plasma pumping as necessary between roll-offs; during plasma pumping, the cathode high voltage is turned off but the cathode is kept near 900°C.

IV.c. Successful Oxide Cathodes

By carefully following the procedure outlined above, this UCD/SLAC collaboration is able to manufacture oxide cathodes with practical work function distributions that peak near 1.625 +/- 0.012 eV. Such cathodes are made using only the 50/50 mix of barium and strontium; traditional oxide cathodes see a work function improvement with the addition of a small amount of calcium. Improved vacuum and

control over the background gases may also yield further improvement on the lowest acheivable work function. Two successful oxide cathodes that were made using the above process are presented here together with roll-offs, practical work function distributions (PWFD's), and residual gas analysis (RGA) data taken during cathode testing.

Cathode BaSr#1 was the first vacuum arc deposited cathode that tested with a work function below 2 eV (previous attempts were deposited using just barium rather than a barium/strontium mix; as is discussed later, exceedingly high water vapor partial pressure was most likely the cause for their high work functions). BaSr#1 began as a 129 nickel button (see description of cathode nickels in Sect. III.a.) that had been laser spot welded onto a package that was assembled using high temperature moly/rhenium braze alloy. Nickel powder had been sprinkled on the face of the cathode and fused to the surface by heating; such a sintering process is common with oxide cathodes in order to help increase the conductivity of the oxide coating thereby reducing stress on the coating during high current operation. This cathode was coated as described above and then activated and tested. It was this cathode that confirmed how low the water vapor partial pressure needed to be in order to achieve a low work function. Initial DC testing revealed a work function just above 2.05 eV as shown in Fig. IV.c.1.

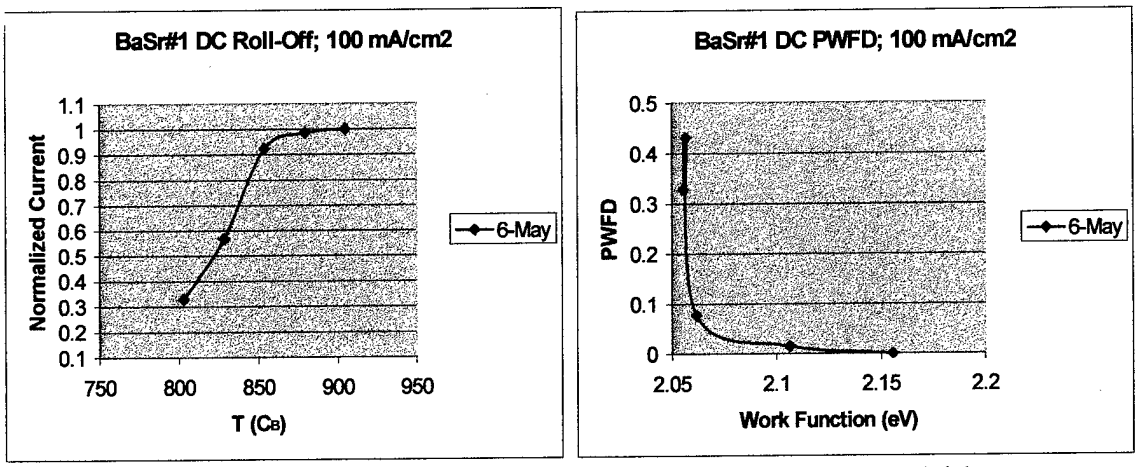

Figure IV.c.1. Initial DC results for cathode BaSr#1 (temperatures on roll-off data are brightness temperatures as explained in Sect. III.d).

During this DC test, total pressure in the vacuum chamber (as measured by the ionization gauge) ranged from 8.2 x 10^{-7} Torr down to 4.4 x 10^{-7} Torr (decreases in cathode current resulted in decreases in pressure due to reduced outgassing via beam interception). The composition of the background gas was also monitored and is shown in Fig. IV.c.2.

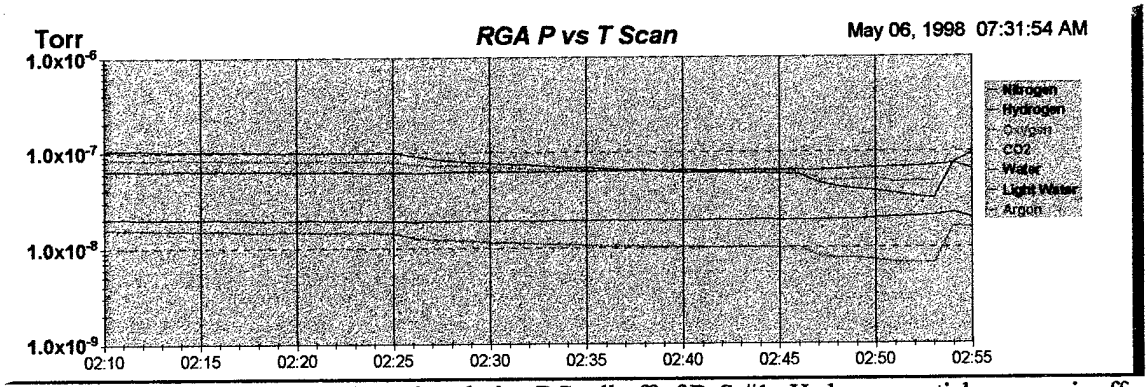

Figure IV.c.2. Strip chart RGA data taken during DC roll-off of BaSr#1. Hydrogen partial pressure is off scale on the positive side, and argon partial pressure is off scale on the negative side.

The first 15 minutes of the scan (from 2:10 to 2:25) correspond to the first three data points on the roll-off where the emission current is still above 9 mA. The decrease in the partial pressures of CO_2, CO (shown as nitrogen above), and O_2 that occur at 2:25

correspond to a 20 minute period when the cathode current dropped from 9.3 mA down to 5.7 mA due to the lowering of the cathode temperature from 855°C to 830°C. The next drop begins at 2:46 when the cathode temperature was reduced to just 800°C accompanied by a drop in emission from 5.7 mA to 3.3 mA. Due to the small thermal mass of the cathode, it can equilibrate to temperature changes on the order of 25°C within 5 minutes at which point the cathode current should stabilize to its temperature limited value. Below 830°C, it was found that the cathode current continued dropping even after 20 minutes, so one may conclude that the cathode surface is poisoning due to the combination of the low cathode temperature and the background gases. At the end of the RGA scan (2:53), the cathode temperature was returned to the starting temperature of 905°C, and the emission readily recovered to 10 mA. To obtain a better picture of the cathode's capabilities, the poisoning had to be reduced by increasing the cathode testing temperatures and removing more of the background gas.

Increasing the cathode roll-off temperatures required operating at emission currents that the DC supply was incapable of driving, so the testing was switched to pulsed mode using the Miram curve generator described in Sect. III.e. A dual roll-off was performed for both 2.5 A/cm^2 and 5.0 A/cm^2 cathode loading with much improved results over the DC tests due to the higher operating temperature of the cathode; the measured work function was now on the order of 1.85 eV. During this dual roll-off the pressure in the chamber ranged from 2.2 x 10^{-7} Torr down to 1.5 x 10^{-7} Torr (lower operating pressure compared to DC testing is due to the reduced average beam power outgassing the chamber surfaces; DC beam power was roughly 3 W compared to the

pulsed average power of less than 0.5 W). Residual gas analysis for this dual roll-off is shown in Fig. IV.c.3.

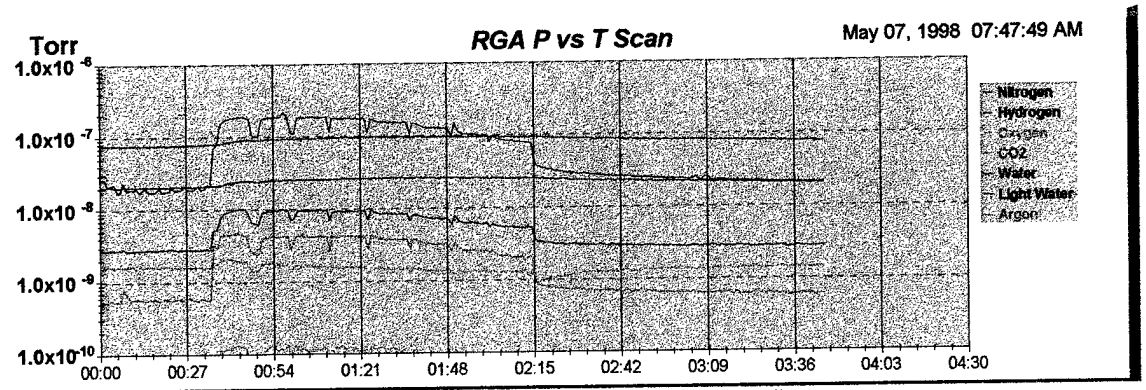

Figure IV.c.3. Strip chart data for initial pulsed emission testing of BaSr#1.

As before, drawing beam current caused the most dramatic changes in the hydrogen, carbon dioxide and carbon monoxide (labeled as nitrogen here) partial pressures. The beam was turned on to 500 mA of current at 00:33 when the roll-off was begun. The dips shown on the traces occurred when the beam voltage was turned down momentarily to collect the 250 mA roll-off data; the beam voltage was immediately returned to the higher value after the current was measured. After the beam was turned off at 2:15, the partial pressures began to slowly return to their pre-test values.

It was at this point that an attempt to improve the background vacuum was made; by firing 200 plasma shots the total pressure in the chamber was reduced from 1.5×10^{-7} Torr to 6.9×10^{-8} Torr. The most dramatic decreases are seen in the partial pressures of water vapor, oxygen, and carbon dioxide as evidenced by Fig. IV.c.4 below.

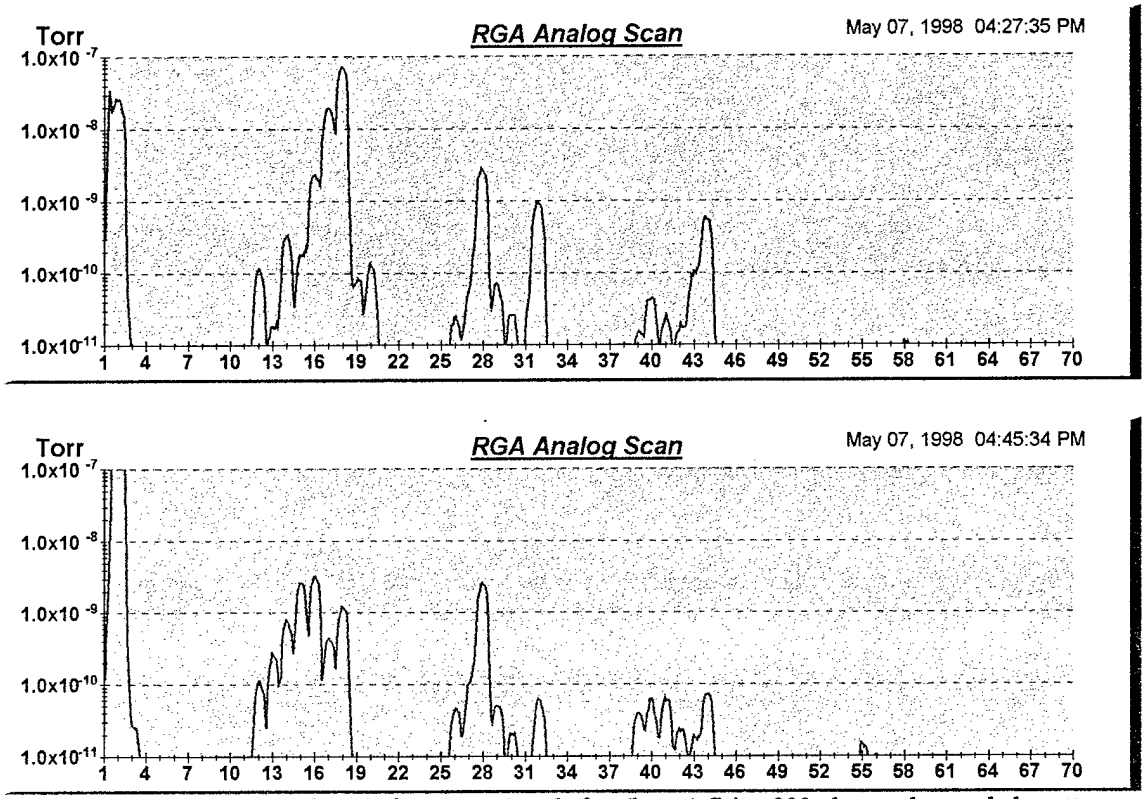

Figure IV.c.4. RGA spectra from before (upper) and after (lower) firing 200 plasma shots to help getter background gases. Hydrogen partial pressure in the lower scan is roughly 2 x 10^{-7} Torr.

Water vapor (18, 17) is decreased by nearly two orders of magnitude while oxygen (32) and carbon dioxide (44) pressures drop by almost an order of magnitude each. Significant hydrogen (2) and methane (13-16) production resulted from firing the plasma. Under such vacuum conditions, the 2.5 A/cm^2 and 5.0 A/cm^2 dual roll-off is repeated with greatly improved results. Shown in Fig. IV.c.5 are the roll-offs and work function distributions for both the pre-plasma pumping and post-plasma pumping data runs.

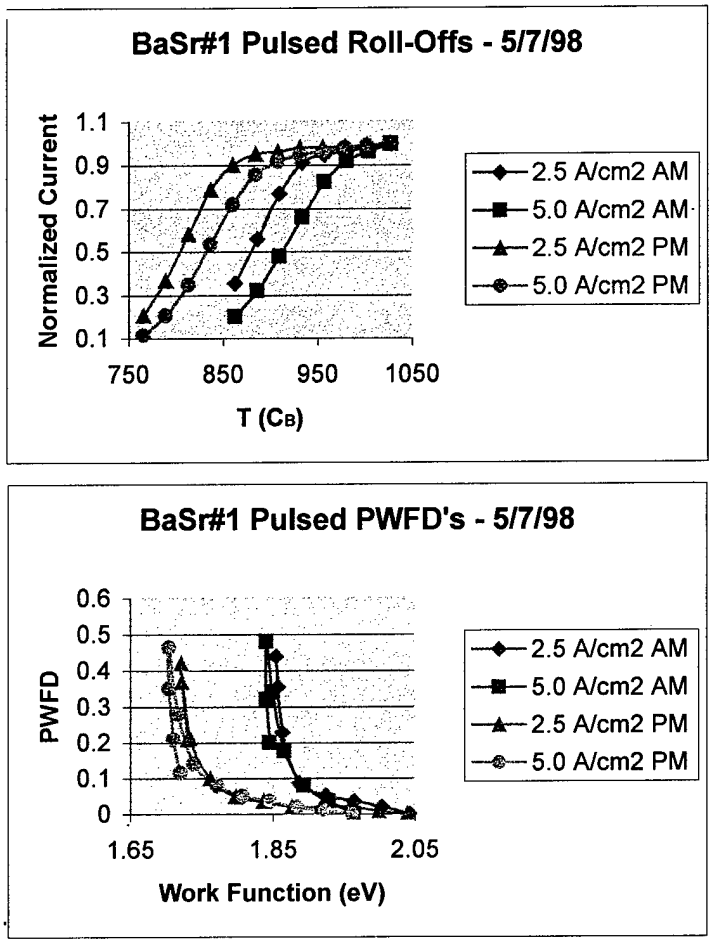

Figure IV.c.5. Emission data for BaSr#1 before (AM) and after (PM) plasma pumping.

In this instance, reducing the background water vapor, oxygen, and carbon dioxide pressures resulted in a drop in the work function from 1.84 eV to 1.70 eV for 5 A/cm^2 cathode loading. Unfortunately, plasma pumping reduces the background gas pressure only temporarily as can be seen from the RGA data taken during this dual roll-off and shown in Fig. IV.c.6.

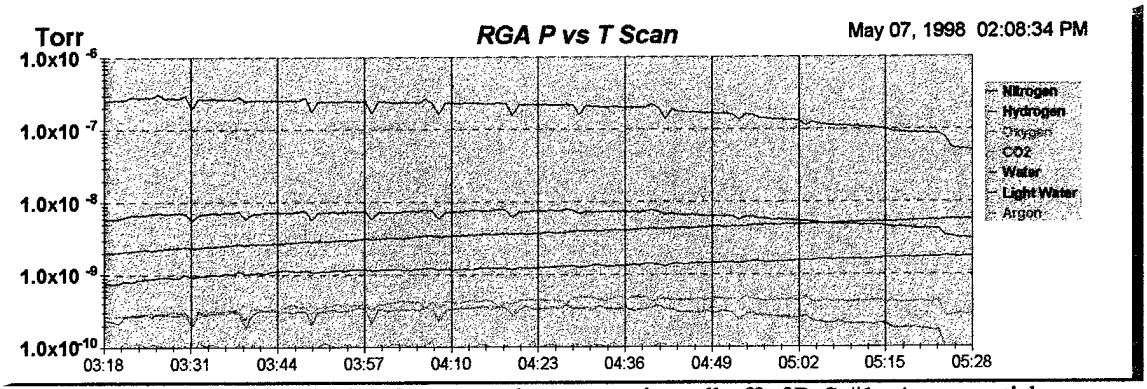

Figure IV.c.6. RGA strip chart data from post-plasma pumping roll-off of BaSr#1. Argon partial pressure is below 10^{-10} Torr.

The dips in the partial pressures of hydrogen, carbon monoxide (labeled nitrogen above), and carbon dioxide are seen as before when the beam voltage is turned down momentarily to measure the 2.5 A/cm^2 loading current. Another significant feature of this scan is the gradual increase of the water vapor partial pressure from its initial value of 2 x 10^{-9} Torr up to 6 x 10^{-9} Torr by the end of the roll-off. This increase is a testament to the fleeting ability of the plasma pumping to reduce the water vapor partial pressure. The resurgence of the water vapor presence seems to be unaffected by the pulsed cathode current since the rise is unchanged when the beam is shut off at 5:23. Due to the improved work function, it was now possible to attempt roll-offs at much higher current densities.

A triple roll-off for current densities of 20, 10, and 5 A/cm^2 was performed while the plasma-pumped water vapor partial pressure was between 1 and 3 x 10^{-9} Torr. Results for this roll-off are given in Fig. IV.c.7.

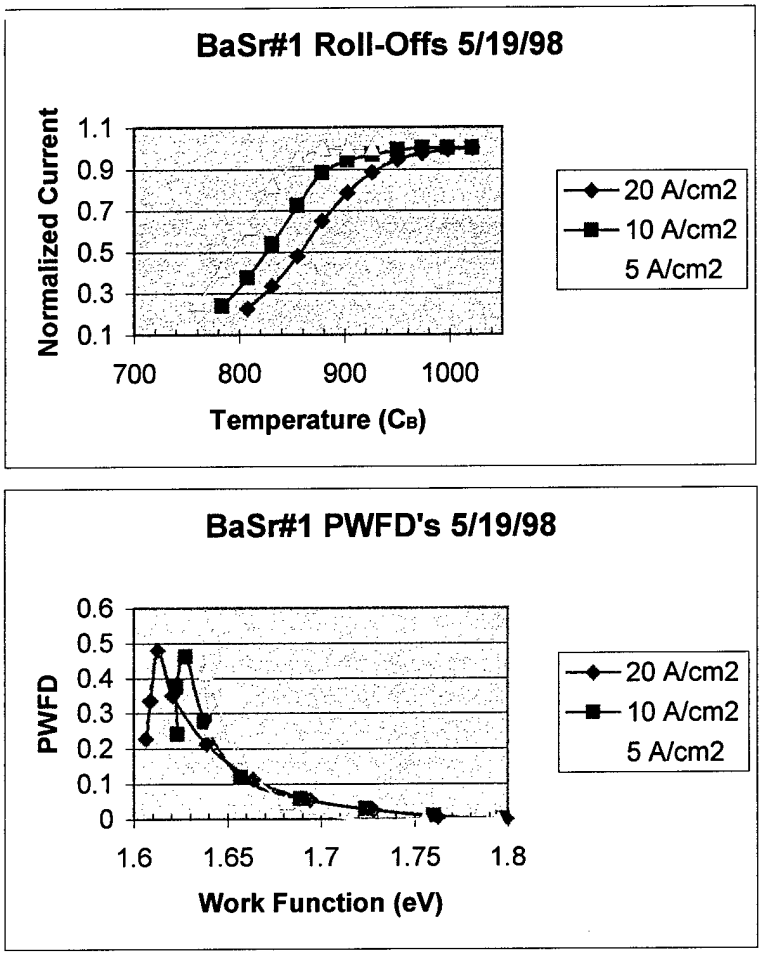

Figure IV.c.7. Pulsed high current density emission data for BaSr#1.

With a work function near 1.6 eV, even higher current densities should be attainable but such roll-offs were prevented by arcing in the cathode package when then applied voltage was increased above 15 kV, the voltage needed to achieve 30 A/cm^2 for this 1.7 μP gun. This cathode emitted 3 A with an applied voltage of 17 kV at a temperature of 1000°C, but arcing prevented the emission from being reliable enough to attempt a roll-off. Given the cathode performance above, a work function of 1.59 eV would lead to emission density of 100 A/cm^2 at only 1000°C, but cathode package arcing prevented such tests.

BaSr#1 was removed from the vacuum chamber and placed in an ultrasonic bath of deionized water. It was discovered earlier that such treatment had a tendency to remove the nickel powder that had been sintered onto the cathode face; in this case, it would remove the oxide coating as well. This freshly cleaned cathode package was then re-installed in the vacuum chamber and promptly baked out using the heater filament. The bare (without sintering) 129 nickel button was then the substrate for the second high performance cathode, BaSr#2.

This second barium/strontium oxide cathode was coated and activated as before and yielded similar results. A DC roll-off was attempted, but it proved to be impossible since the low operating temperature of the cathode (~740°C) allowed poisoning even when the background gas had been plasma pumped with the water vapor partial pressure near 7×10^{-9} Torr. The switch was made to pulsed testing with the results as given in Fig. IV.c.8.

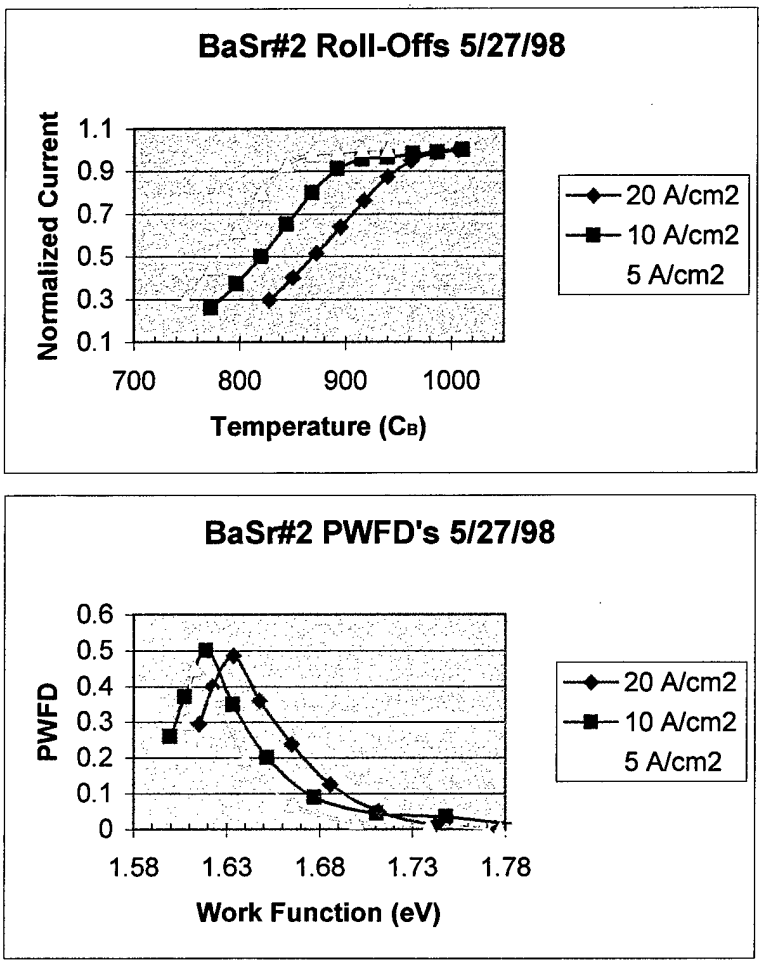

Figure IV.c.8. Pulsed high current density emission data for BaSr#2.

Background gas partial pressures during the 20 A/cm^2 roll-off are shown in Fig. IV.c.9.

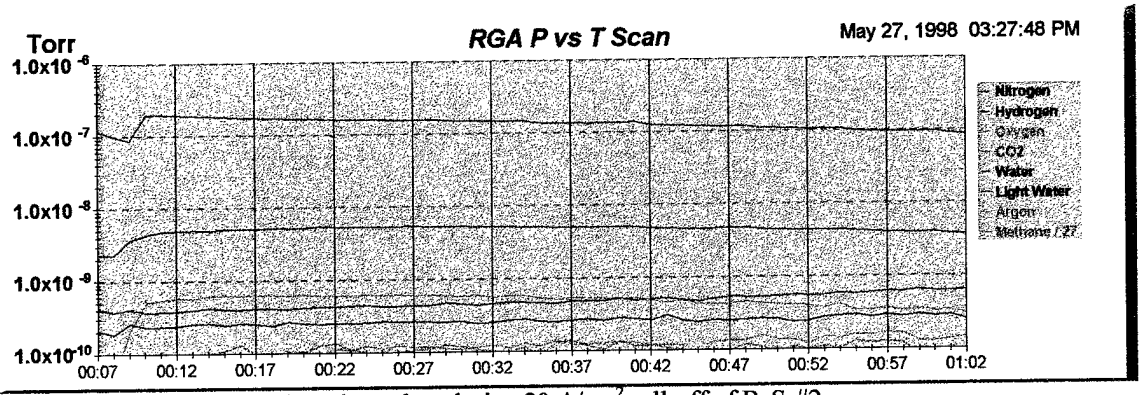

Figure IV.c.9. RGA strip chart data taken during 20 A/cm^2 roll-off of BaSr#2.

The RGA strip chart shows the increase in gas partial pressures when the cathode current is turned on at 00:09. Dips are not observed in the gas pressures during the roll-off since the voltage was held constant for this 20 A/cm^2 roll-off. Over the course of the roll-off, the water vapor partial pressure rose gradually from 4 to 7 x 10^{-10} Torr. Similar RGA data was taken for the dual 10 and 5 A/cm^2 roll-off performed and is shown in Fig. IV.c.10.

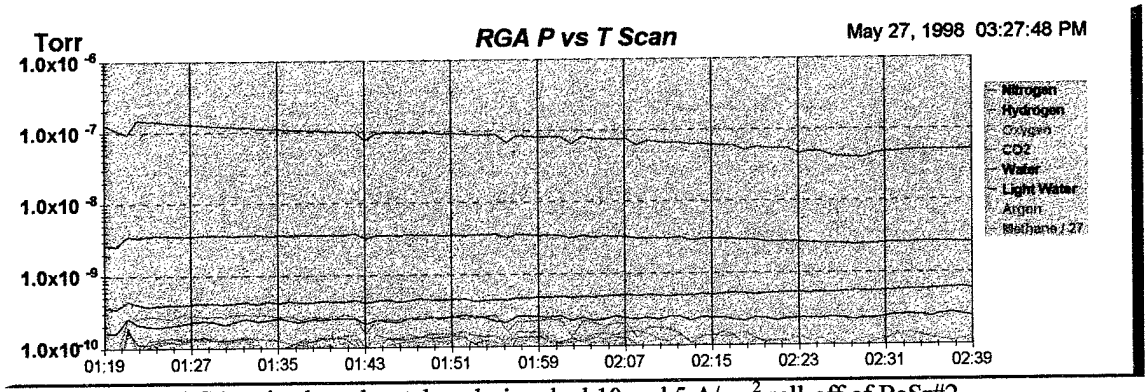

Figure IV.c.10. RGA strip chart data taken during dual 10 and 5 A/cm^2 roll-off of BaSr#2.

Dips are evident in the gas partial pressures during the momentary drop in voltage when the emission for the 5 A/cm^2 roll-off is measured. Again, arcing in the cathode package prevented testing the cathode at higher current densities.

The closely matched performance of BaSr#1 and BaSr#2 prove the viability of using the vacuum arc deposition technique for manufacturing oxide cathodes with work functions near 1.6 eV (with the eventual goal of reducing the workfunction to as low as 1.3 eV to match the performance of the very best oxide cathodes). The slight variations in the work function for the different emission densities may be reduced by improving the vacuum environment during both coating and testing as well as by increasing the uniformity of the coating by using a macroparticle filter as described in Sect. II.b. Unfortunately, lack of control of the background gases can lead to a significant performance reduction as is described in the next section.

IV.d. Unsuccessful Oxide Cathodes

Before the barium/strontium mixed plasma sources were available, initial oxide cathodes were made using a pure barium plasma. These first few attempts at making an oxide cathode proved unsuccessful most likely due to insufficient vacuum. BaO#1 showed no emission whatsoever most likely due to the lack of cathode heating during air exposure; in the presence of the water vapor in air, any deposited oxides were most likely converted to hydrates of barium hydroxide via[6]

$$BaO + n \cdot H_2O \rightarrow Ba(OH)_2 \cdot (n-1)H_2O\,.$$

The excess water molecules poison the cathode emission by converting the oxide coating into a hydroxide coating and its various hydrates which no longer share the oxide coating's attractively low work function. Subsequent cathodes still poisoned very easily in the presence of high water vapor partial pressure, as is evidenced by the roll-off data shown in Fig. IV.d.1.

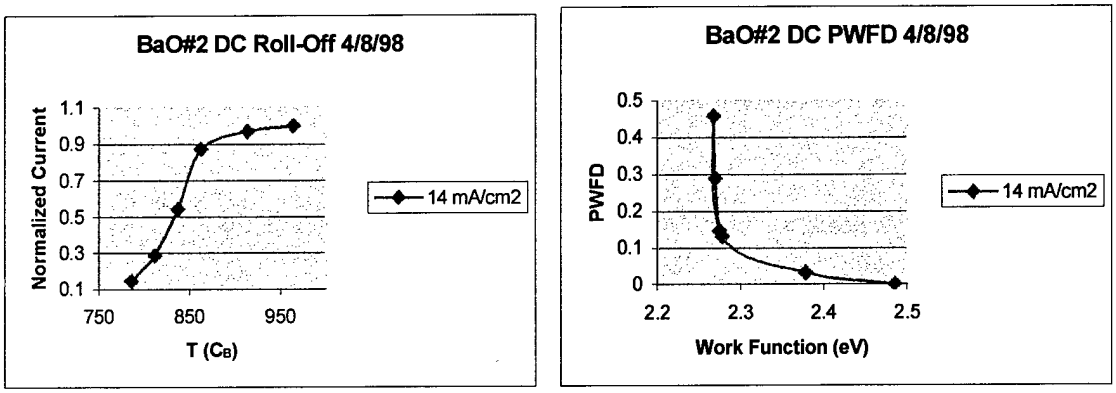

Figure IV.d.1. DC emission test for BaO#2.

Even at a temperature of 950°C, space charge limited emission was only possible below 1.5 mA due to the high work function brought on by poisoning. The partial pressure of water vapor during this test was approximately 1 x 10^{-7} Torr (this test was performed before implementing plasma pumping to reduce the water vapor partial pressure). To ensure that the coating was not contaminated, Rutherford backscattering spectroscopy (RBS) and x-ray photoelectron spectroscopy (XPS) were performed on two separate samples. The RBS data which examined the surface of BaO#2 (sintered 129 nickel base) after it was removed found only barium, hydrogen, and oxygen (detection limits for elements $16<Z<92$ is 0.5 atomic percent; carbon detection limits are much worse). These results indicated that there were no gross impurities in the source rods, but it was still

undertermined what chemical form the coating was in—likely candidates include carbonates, hydroxides, hydrates and oxides. XPS data taken on one of the source rods showed barium oxides, barium carbonates, and other hydrocarbons. The barium compounds were readily converted to atoms and ions during the plasma generation, so the presence of oxides and carbonates was not alarming. However, the hydrocarbons are a possible source of poisoning for the cathode and their presence suggests that a better method for making and storing the barium/strontium-filled nickel tubing may need to be found in the future to achieve the lowest possible work functions.

BaO#3 (bare 129 nickel base) suffered from the same poor vacuum as BaO#2. Water vapor partial pressure was roughly 9 x 10^{-8} Torr during the test shown below in Fig. IV.d.2.

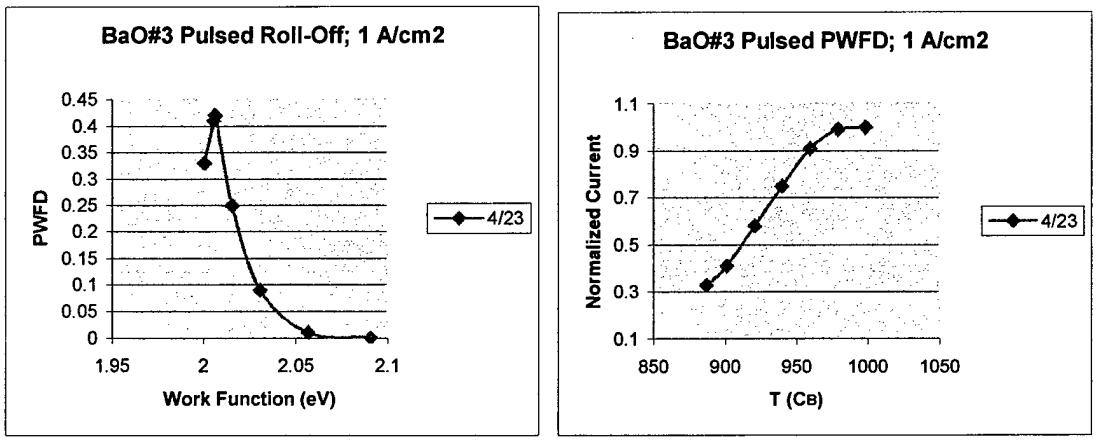

Figure IV.d.2. Pulsed emission data for background water vapor partial pressures of 9 x 10^{-8} Torr.

At this point in the experiment, the mixed barium/strontium source rods became available, and a higher temperature braze material was now being used in assembling the cathode packages (previous packages were assembled using a copper/gold braze that was evaporating heavily during cathode testing due to the high temperature of the cathode

package). The next two cathodes made and tested were BaSr#1 and BaSr#2 which were described in the previous section. Following the success of those two cathodes, further attempts at successful cathodes were made but with unreliable results.

BaSr#3 (bare 230 nickel base) was an attempt to improve the perveance of the gun by forcing the cathode and anode packages together using tension in a nichrome wire that held them together. Unfortunately, this process of joining the cathode and anode packages with a twisted wire required more than fifeteen minutes during which time the coated cathode was exposed to air. Upon heating the cathode, it was found that one side of the cathode face was held in contact with the focus electrode which acted as a heat sink. As such, uniform heating of the cathode surface could not be achieved so the cathode had to be exposed to air yet again to re-dock the packages. The cathode perveance did indeed improve, but the additional air exposure caused fracturing and flaking of the coating. The flaking was most likely due to the absorption of large amounts of water vapor which then poisoned the emission to the point where no roll-offs were possible. Upon removal from the chamber, the surface of the cathode was analyzed under a microscope and compared to such analysis of other cathodes. Sample photos of three cathode surfaces are shown in Fig. IV.d.3.

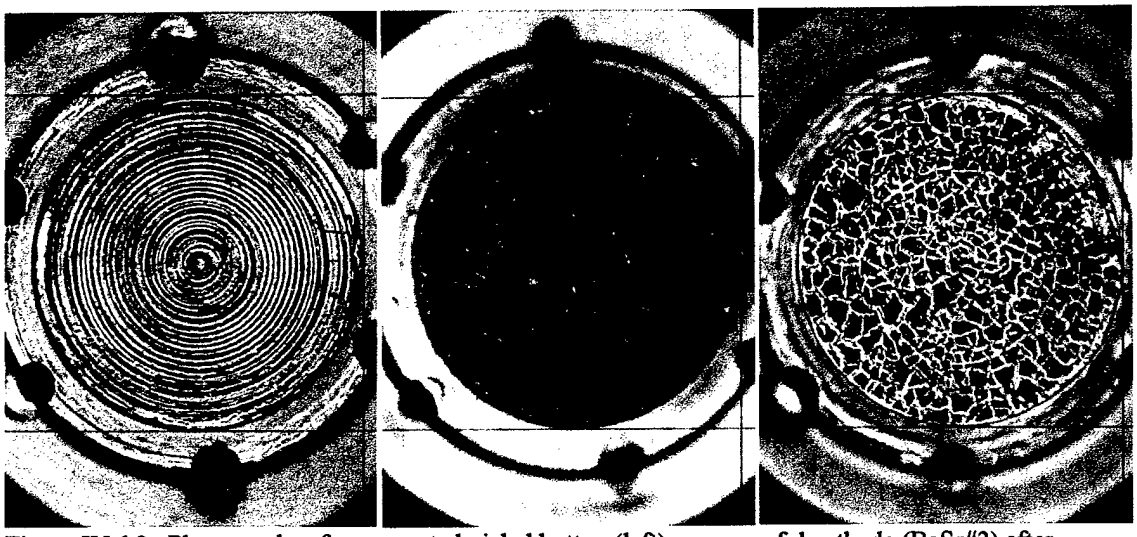

Figure IV.d.3. Photographs of an uncoated nickel button (left), a successful cathode (BaSr#2) after removal, and an unsuccessful cathode (BaSr#3) after removal. Each cathode is 3.58 mm in diameter.

Even the successful cathode shows some signs of cracking, but these fissures were most likely formed after removing the cathode from the vacuum chamber. The flaking of BaSr#3's coating was evident even in vacuum when the cathode surface was glowing, so the damage to the coating was already present before removal.

BaSr#4 (bare 129 nickel base) was an attempt at rapidly making and testing a successful oxide cathode. The poor performance of this cathode is a testament to the high vacuum required for the successful manufacture of an oxide cathode. This cathode was coated when the water vapor partial pressure was still above 1×10^{-6} Torr. Even after the chamber had been allowed to pump for two days and the water vapor partial pressure was brought into the low 10^{-9} Torr scale via plasma pumping, this cathode retained a high work function as can be seen in Fig. IV.d.4.

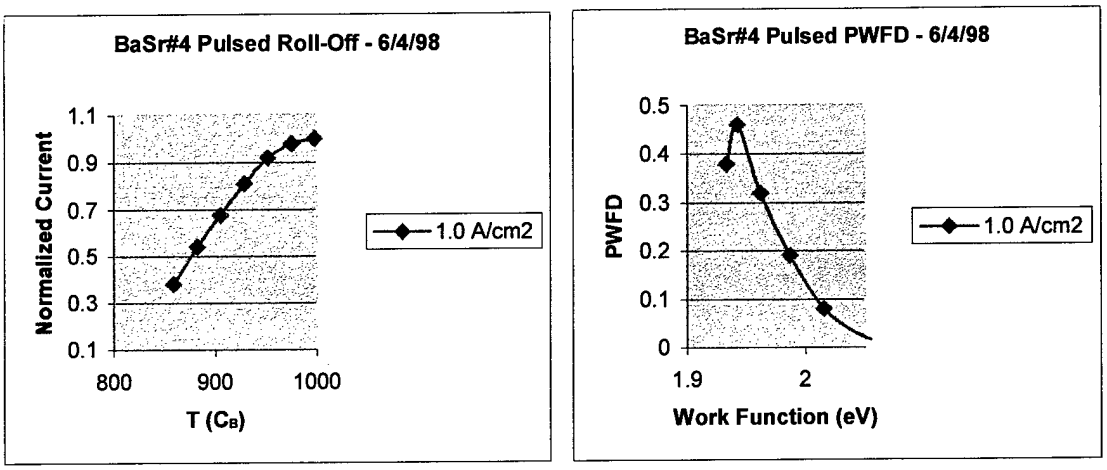

Figure IV.d.4. Pulsed emission data for BaSr#4.

This cathode emphasized the importance of achieving a good vacuum not only for the testing procedure but also for the deposition of the oxide coating. This lesson having been learned, the final cathode in the current work, BaSr#5 (bare 230 nickel base), was prepared.

The partial pressure of water vapor at the beginning of the deposition for BaSr#5 was less than 8×10^{-8} Torr. The coating process went smoothly and was followed by a docking process during which the cathode was exposed to air (while kept warm) for only 3 minutes. The chamber was then allowed to pump for 3 days before cathode activation was begun. Water vapor partial pressure was below 2×10^{-8} Torr during the initial heating of the cathode, and climbed as high as 6×10^{-8} Torr once the beam was turned on. The DC I-V characteristic of the cathode appeared extremely space charge limited at a cathode temperature of 910°C, so the switch to pulsed testing was made. Unfortunately, after this switch was made, the emission of the cathode dropped significantly. This unexpected decrease in cathode performance led to the decision to go back to DC testing

to determine if the previous characteristics could be recovered. This sudden loss of cathode performance is documented in Fig. IV.d.5.

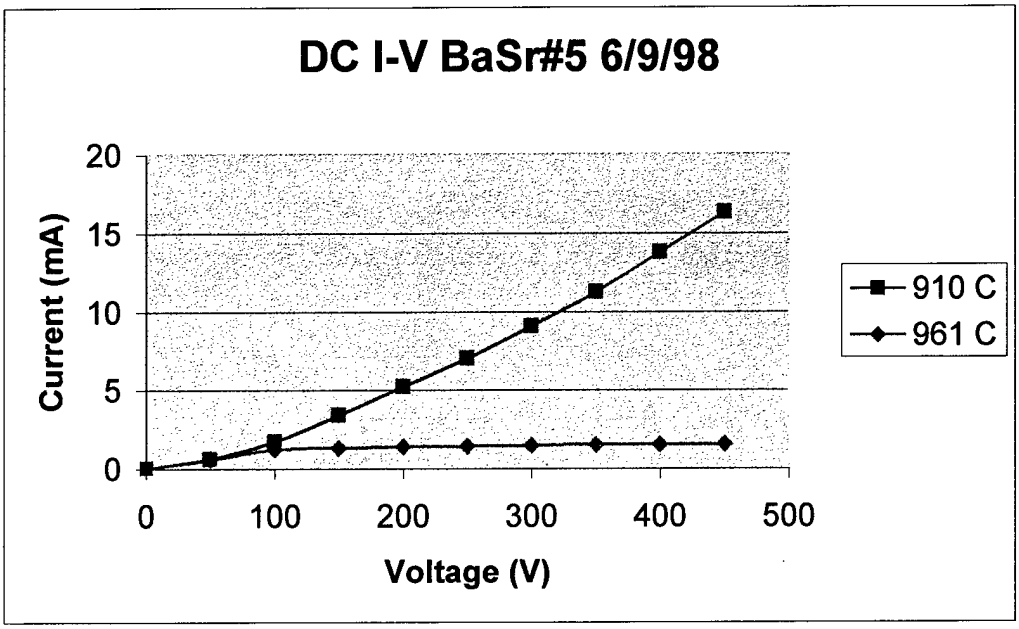

Figure IV.d.5. DC emission data taken before (910°C) and after (961°C) switching to the pulsed power supply.

Even after applying additional heat to the cathode and plasma pumping to reduce the background water vapor partial pressure below 1 x 10^{-9} T, acceptable emission could not be recovered. Thus, it is seen that even under good vacuum conditions, the air exposure that the cathode must undergo to dock it into the anode structure is sufficient to prevent repeatable, reliable cathode performance. Nevertheless, vacuum arc deposition was shown capable of producing oxide cathodes with work functions significantly lower than today's standard dispenser cathodes (1.8 eV). Such oxide cathodes should be capable of emission densities on the order of 100 A/cm^2 once the problem of arcing inside the cathode/anode package is solved.

V. CONCLUSIONS & SUMMARY

Vacuum arc deposition has proven to be a novel, viable method for making oxide cathodes without the introduction of adhesives or binders that may later poison the cathode. In addition, the carbonate conversion/activation process may be nearly eliminated by depositing the coating in the presence of oxygen as long as there is a lack of available carbon to form any carbonates. These oxide cathodes are still very much in their infancy, and there may still be significant work function improvements ahead if greater control over the process cleanliness can be achieved.

In pursuit of the ultimate goal of a repeatable, reliable process for making an oxide cathode capable of emitting 100 A/cm^2, an evacuated transfer vessel is being manufactured at SLAC that will allow the user to coat an oxide cathode in the deposition chamber and subsequently transfer the cathode to a separate analysis chamber without ever exposing the cathode to ambient air. This vessel and its counterparts which mount inside the deposition and analysis chambers are still many months away from completion. Once the transfer vessel is in operation, transferring the coated cathode to a cleaner chamber for analysis will remove the detrimental air exposure from the process steps. In addition, the lower base pressure of the analysis chamber will provide a more accurate picture of the best work function attainable with these oxide cathodes. The correlation shown in Sect. IV.c. and IV.d. between increasing water vapor pressure and decreasing cathode performance provides convincing evidence for the importance of reducing the

presence of water vapor in not only the analysis chamber but the deposition chamber as well.

To help achieve a lower water vapor partial pressure, ultra-violet lamps will be installed in the deposition chamber. Water molecules adsorbed on metal surfaces may be liberated from the surface given the energy of a UV photon. Such water molecules may subsequently be pumped out and removed from the vacuum system. Once this system is installed, it is expected that water vapor will be pumped much more readily and to a much lower base level.

Another improvement to the ultimate base pressure of the deposition system may be made by replacing the Viton o-ring seal at the chamber lid with a metal seal such as a helicoflex gasket. Improving the pre-deposition base pressure is expected to reduce the amount of carbon monoxide and carbon dioxide available so that the coating will be deposited as an oxide rather than a carbonate. The evolution of carbon dioxide seen during initial cathode heating (see Fig. IV.b.1.) implies the presence of at least a partially carbonated coating. If one can restrict the available carbon gases to the point that the coating is deposited as a pure oxide, then one eliminates both the conversion process and the accompanying density change which may impair film adhesion. By using a metal seal at the lid, one removes the source of gas that a Viton o-ring becomes at pressures in the low 10^{-8} T scale (in this pressure range, Viton outgasses and becomes slightly permeable).

Once the cathode emission and work function results are consistent from cathode to cathode, other variables may be introduced to see how they affect cathode

performance. Adding a small amount of calcium to the barium/strontium source rods is expected to yield a slight reduction in the work function of the cathode (traditionally manufactured oxide cathodes found their best performance when small amounts, i.e. a few percent by atomic ratio, of calcium were added to the coating). Depositing a thicker coating will definitely improve the lifetime of the cathode (it will take more time for all of the barium/strontium/calcium to evaporate), but it may also increase the work function due to the increased amount of time it will take for free barium to diffuse from the oxide/nickel interface to the surface of the cathode (a layer of free barium on the surface of an oxide cathode is believed to play an important role in the low work function of the cathode[1]).

In the separate cathode analysis chamber, a 3-D beam analyzer will also be available that will be able to profile the current density across the surface of the cathode. Such analysis will help determine if there are any "dead" spots on the cathode surface by checking for emission uniformity. If it is found that the emission uniformity is poor, a macroparticle filter (as described in Sect. II.b) may be added to the deposition process so that only ionized atoms reach the substrate thereby forming a much smoother, more uniform coating.

If the oxide film shows a tendency to flake off under the stress of operating with higher current densities, the energy with which the ions impact the nickel substrate may be varied in order find an optimal implantation energy. Tailoring the implantation energy up or down may affect how well the oxide film is bonded to the nickel substrate.

Lastly, the amount of oxygen needed to oxidize the film during deposition has yet to be determined. Ideally, the oxide should be formed during the brief (~1 sec) interval between plasma shots so that the coating is deposited as an oxide rather than as a pure metal coating that is converted to an oxide by subsequent oxygen absorption and diffusion throughout the film. By forming the oxide layer by layer, one may prevent any sudden density and/or volume changes in the coating that might occur if the metal is converted to an oxide after the entire coating is finished. As such, the partial pressure of oxygen present during the deposition should be adjusted up and down to determine its optimal value.

Following the improvements outlined above, vacuum arc deposition may become a repeatable, reliable method for manufacturing an oxide cathode that outperforms all dispenser cathodes (the most popular cathode for linear tube devices today) at a fraction of the manufacturing costs. For example, the Next Linear Collider for high enery experimental physics in its current design would require 4,000 to 8,000 high power microwave klystrons. By reducing the cost of the cathode employed inside each tube from $4k for a dispenser cathode to under $1k for a vacuum arc deposited oxide cathode, one may potentially save up to $24M in costs. Additional applications for these oxide cathodes may be found not only in linear collider klystrons but also in high power microwave directed energy weapons, cancer treatment klystrons, satellite communications travelling wave tubes, monitor CRT's, and even fluorescent lamps.

REFERENCES

I. INTRODUCTION

1. A. W. Wright, *The American Journal of Science and Arts* **13**, 49 (1877)
2. T. A. Edison, US Patents 484,582 (1892) and 526,147 (1894)
3. L. P. Sablev, et al., U.S. Patents 3,793,179 and 3,783,231 (1974)
4. **Handbook of Vacuum Arc Science and Technology**, edited by R. L. Boxman, P. J. Martin, D. M. Sanders (Noyes, New Jersey, 1995)
5. H. C. Miller, "A Bibliography and Author Index for Electrical Discharges in Vacuum (1897-1986)", General Electric Co., document No. GEPP-TIS-366e (UC-13), 1988; also published in part in *IEEE Transactions on Electrical Insulation* **25**, 765 (1990) and **26**, 949 (1991)
6. A. Wehnelt, *Sitzungsberichte der Physikalisch-medizinischen Sozietat zu Erlangen* **95**, 115 (1903)
7. A. Wehnelt, *Verhandlungen der Deutschen Physikalischen Gesellschaft* **5**, 346 (1903)
8. A. Wehnelt, *Annalen der Physik* **14**, 425 (1904)
9. **Sperry Electronic Tube Manual**, 17.20 (1958)
10. M. Cattelino, G. Miram, *Applied Surface Science* **111**, 90 (1997)
11. From private communication with Dr. R. T. Longo of Hughes and the publication R. Loosjes, H. J. Vink, *Philips Research Report* **4**, 449 (1949)
12. Improved electrical conductivity of molecularly-deposited coating: Yu. A. Kondrashenkov, L. A. Yumasheva, *Bulletin of the Academy of Sciences of the U.S.S.R. Geophysics Series* **40**(12), 16 (1976)
    Emission uniformity of molecularly-deposited cathode: A. V. Druzhinin, Yu. A. Kondrashenkov, *Radio Engineering and Electronic Physics* **18**, 1134 (1973)
    Robustness of a pressed porous oxide cathode: K. P. Rybas, V. K. Pavlov, B. N. Telepaev, *Instruments and Experimental Techniques* **16**, 1756 (1973)

II. MANUFACTURING APPARATUS

1. Y. Ji, T. Wu, *Journal of Vacuum Science and Technology A* **6**, 1073 (1988)
2. I. G. Brown, J. E. Galvin, R. A. MacGill, *Applied Physics Letters* **47**, 358 (1985)
3. I. G. Brown, A. Anders, S. Anders, M. R. Dickinson, R. A. MacGill, *Journal of Vacuum Science and Technology B* **12**, 823 (1994)
4. I. G. Brown, A. Anders, S. Anders, M. R. Dickinson, R. A. MacGill, O. Monteiro, E. M. Oks, S. Raoux, Z. Wang, G. Yushov, *Materials Research Society Symposia Proceedings* **396**, 467 (1996)
5. **Handbook of Vacuum Arc Science and Technology**, edited by R. L. Boxman, P. J. Martin, D. M. Sanders (Noyes, New Jersey, 1995)

6. R. A. MacGill, M. R. Dickinson, A. Anders, O. R. Monteiro, I. G. Brown, *Review of Scientific Instruments* **69**, 801 (1998)
7. W. J. Corbett, Master's Thesis entitled "Initial results from the Toroidal Cusp Experiment-II," Univerity of California (1987)
8. A. Anders, S. Anders, I. G. Brown, M. R. Dickinson, R. A. MacGill, *Journal of Vacuum Science and Technology B* **12**, 815 (1994)

III. ANALYSIS APPARATUS

1. The development of the emission law follows that given in **Theory and Design of Charged Particle Beams**, M. Reiser (John Wiley & Sons, New York, 1994).
2. For the complete prescription for generating a practical work function distribution, see M. Cattelino, G. Miram, *Applied Surface Science* **111**, 90 (1997).

IV. RESULTS & DISCUSSION

1. M. Kuhn, R. Pintaske, F. Richter, *Proceedings: ISDEIV, XVIIth International Symposium on Discharges and Electrical Insulation in Vacuum, Berkeley, California, July 21-26, 1996* **1**, 932 (1996)
2. C. Bergman, *Surface and Coatings Technology* **36**, 243 (1988)
3. P. J. Martin et al., *Journal of Vacuum Science and Technology A* **5**, 22 (1987)
4. Z-Y. Cheng, J-Y. Zou, L. Yang, *Proceedings: ISDEIV, XVIIth International Symposium on Discharges and Electrical Insulation in Vacuum, Berkeley, California, July 21-26, 1996* **1**, 858 (1996)
5. Y. Ji, T. Wu, *Journal of Vacuum Science and Technology A* **6**, 1073 (1988)
6. Y. Ji, T. Wu, *Journal of Vacuum Science and Technology A* **6**, 1073 (1988)

V. CONCLUSIONS & SUMMARY

1. From private communication with Dr. R. T. Longo of Hughes and the publication R. Loosjes, H. J. Vink, *Philips Research Report* **4**, 449 (1949)